SOME FACTORS INFLUENCING THE STRESS-STRAIN BEHAVIOUR OF CLAYS

by

A.S.BALASUBRAMANIAM

VOLUME III

Figures

Chapters 5 to 8

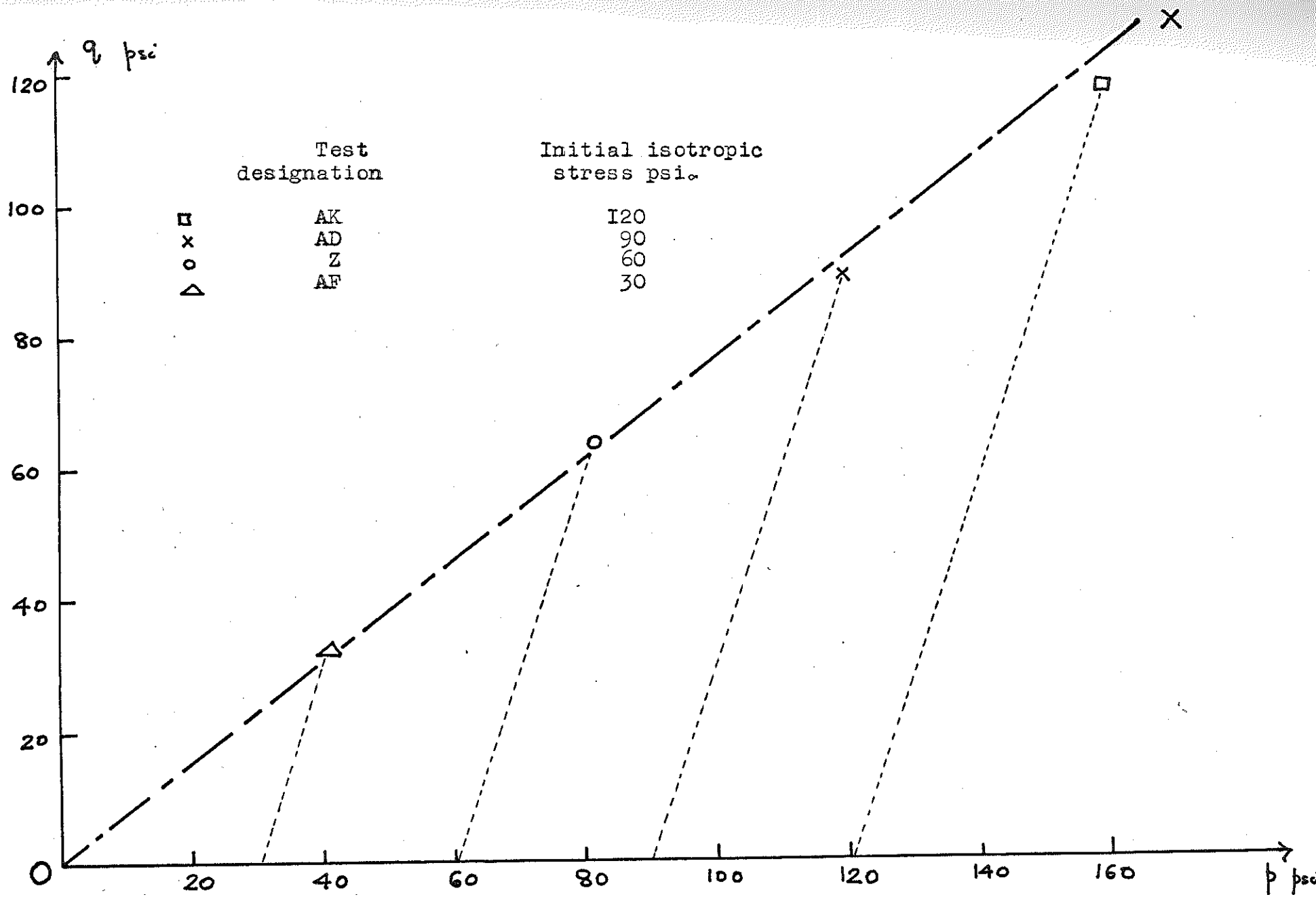

Fig. 5.I The peak stress points in (q, p) space of four fully drained tests with constant cell pressure.

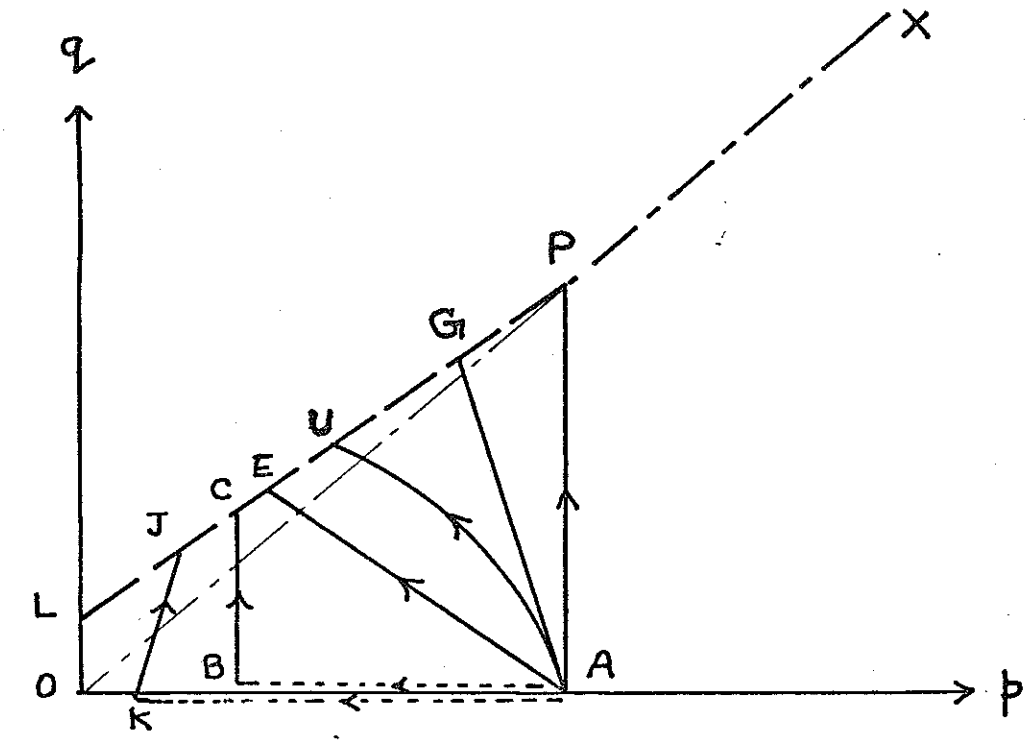

(a)

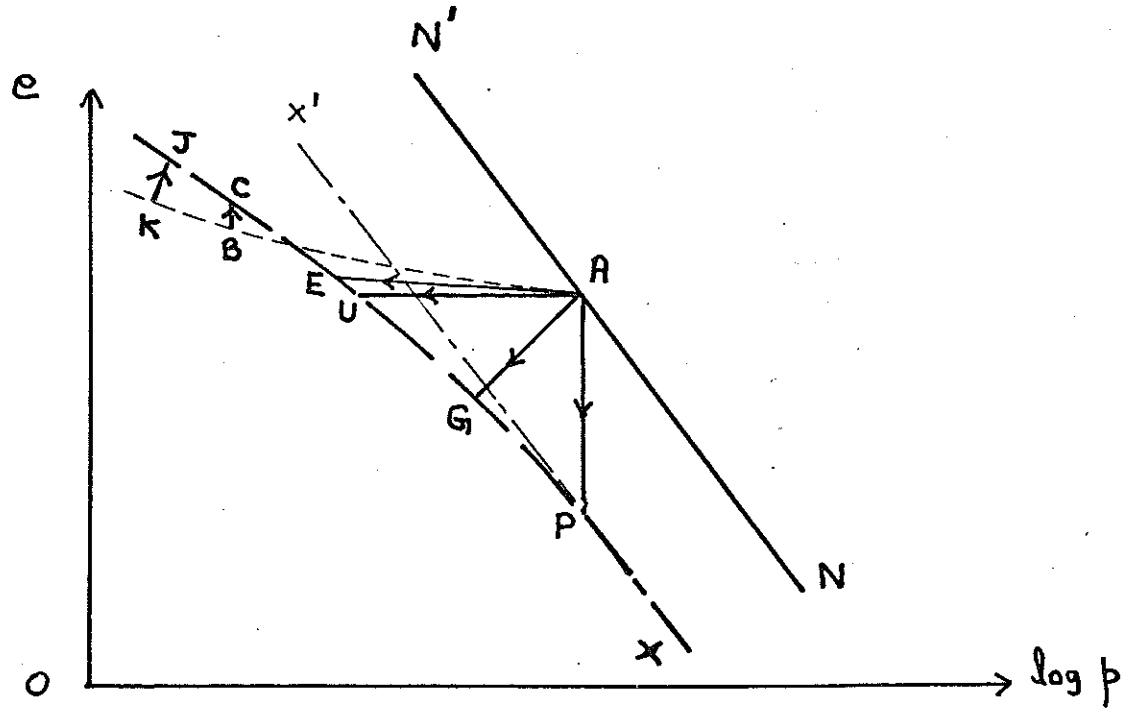

(b)

Fig. 5.2. The paths followed by specimens in Type I tests, in (a) the (q,p) space and (b) the (e, log p) space

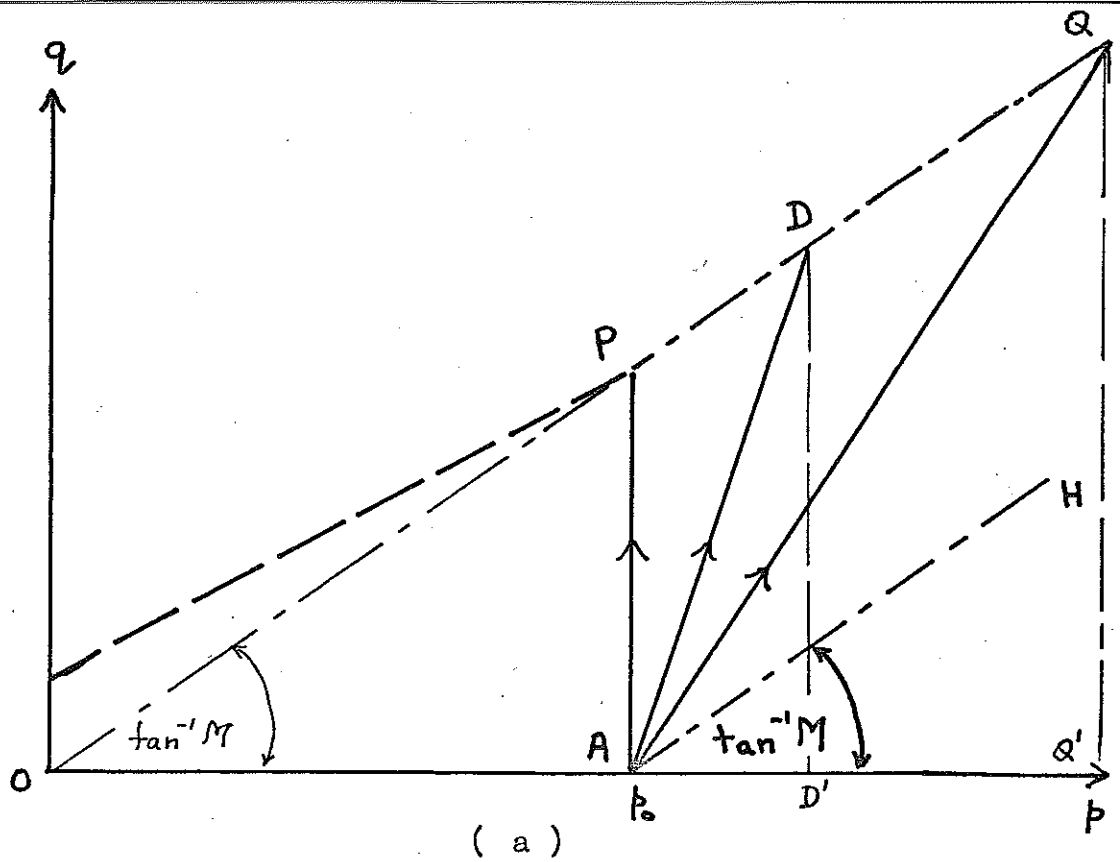

(a)

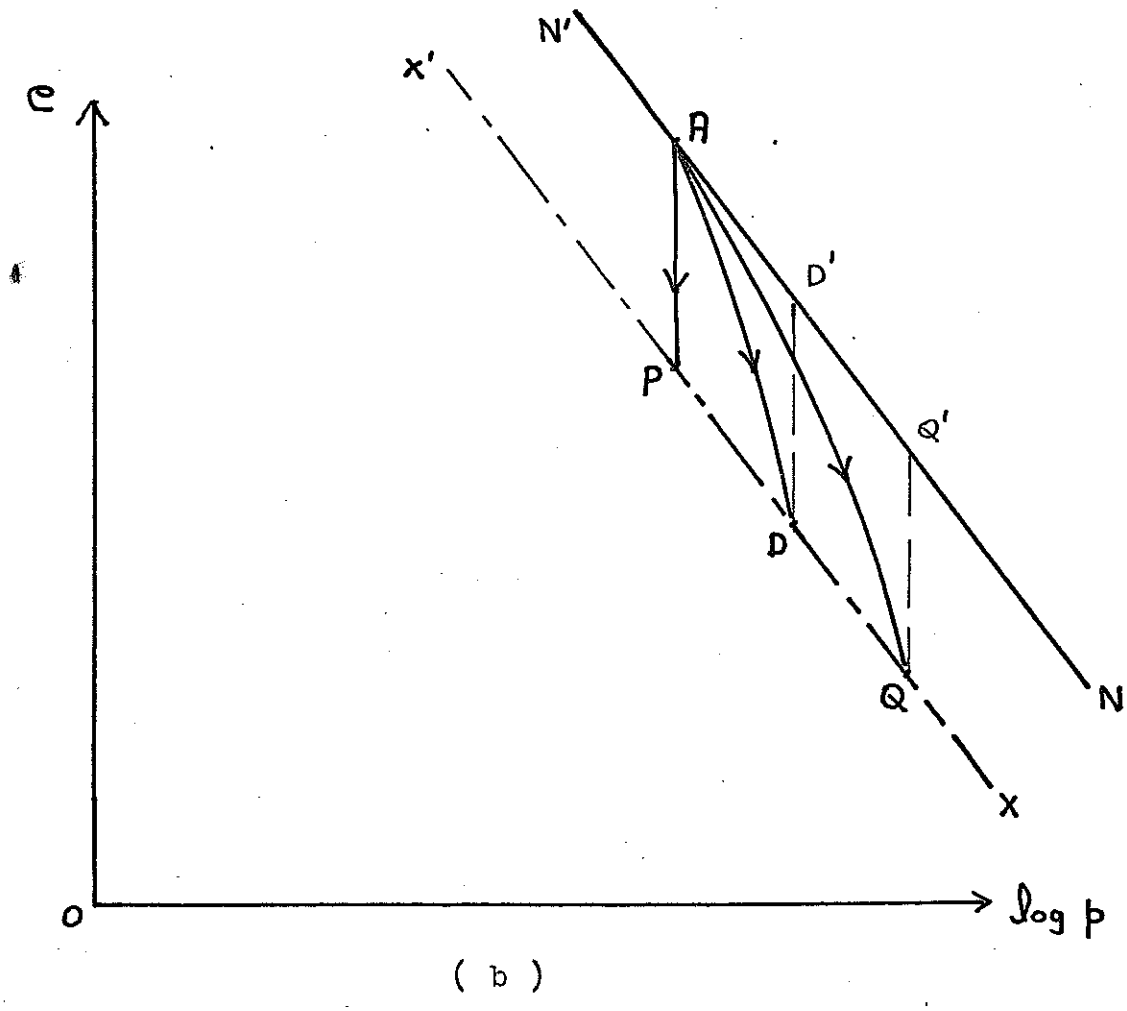

(b)

Fig. 5.3. The paths followed by specimens in Type 2 tests, in (a) the (q,p) space and (b) the (e, log p) space

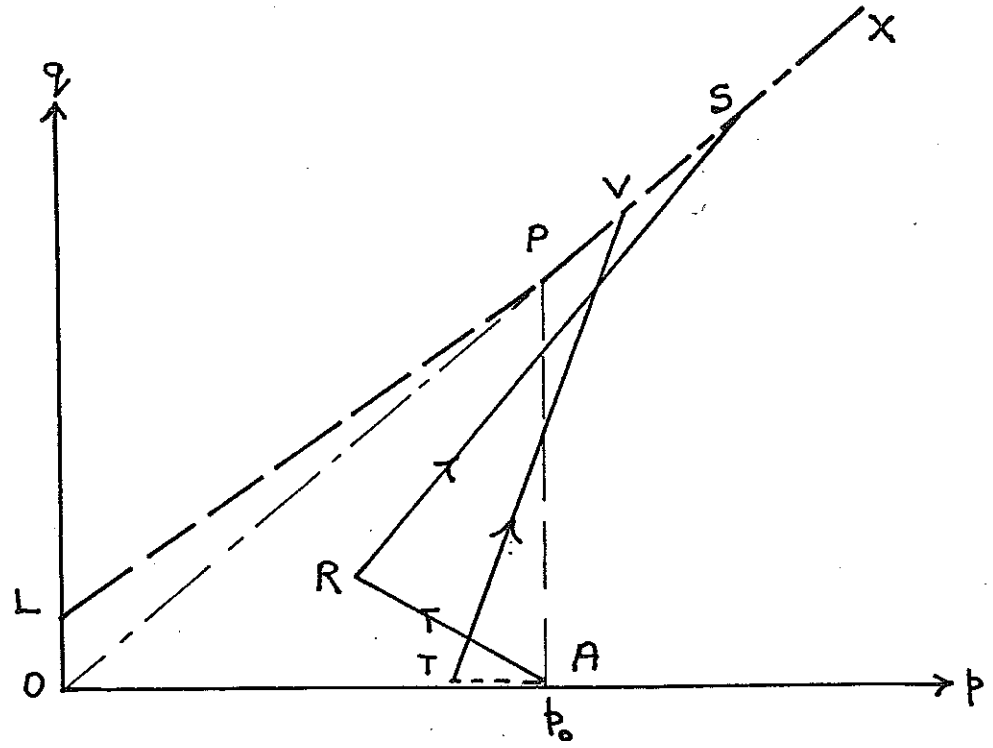

(a)

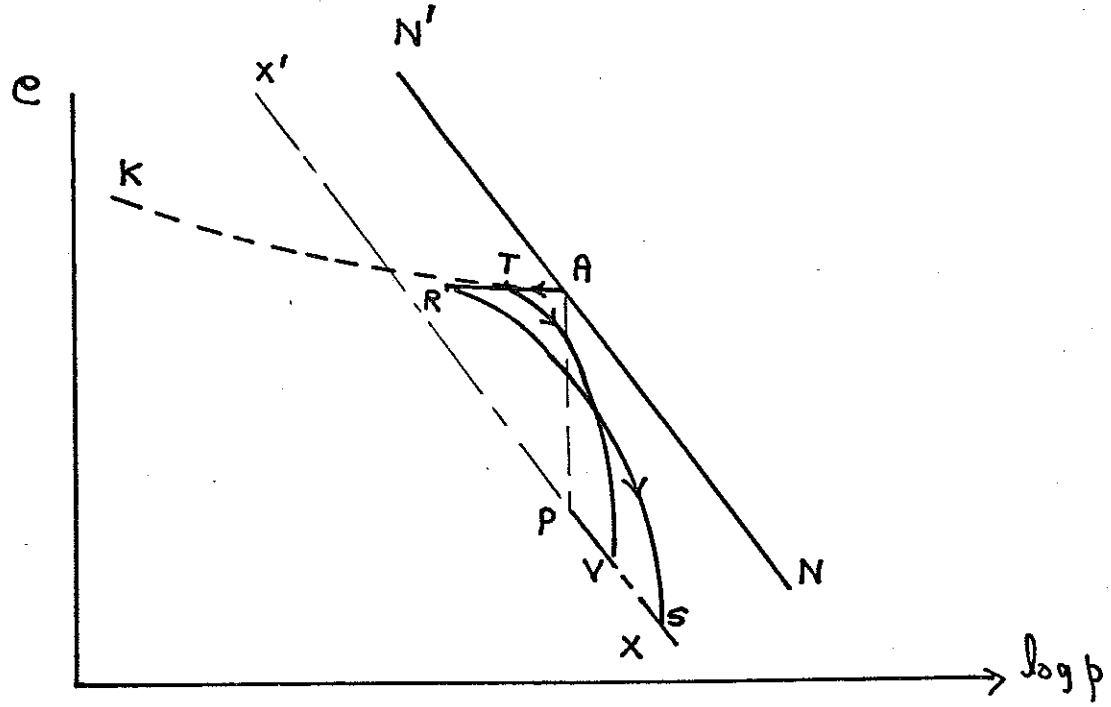

(b)

Fig. 5.4. The paths followed by specimens in Type 3 tests in (a) the (q,p) space and (b) the (e, log p) space.

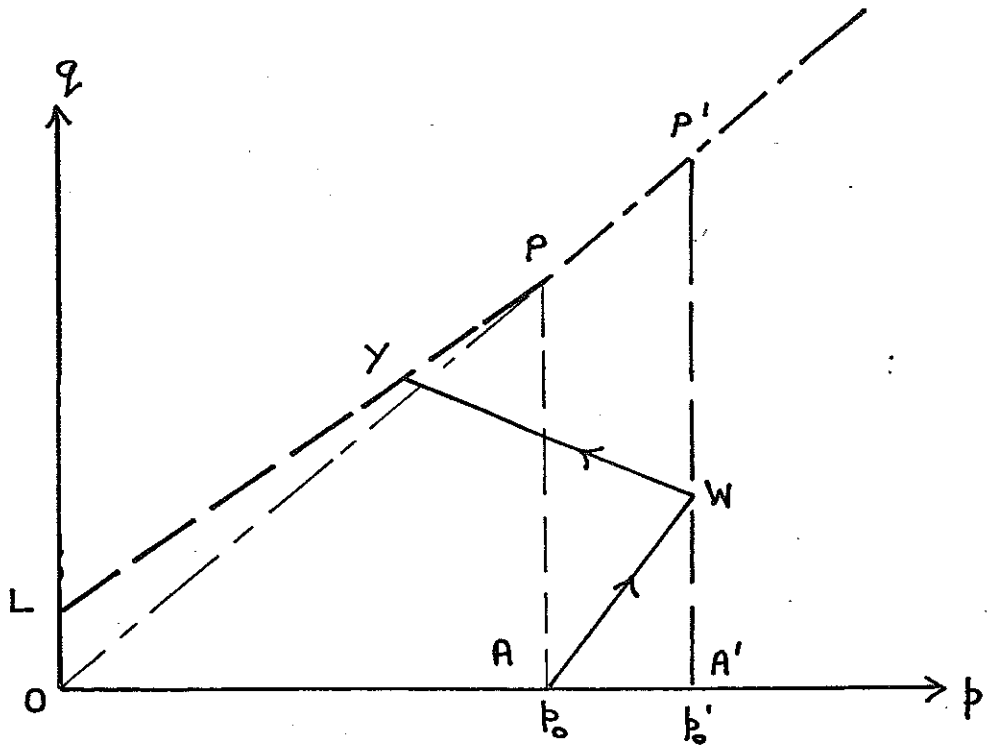

(a)

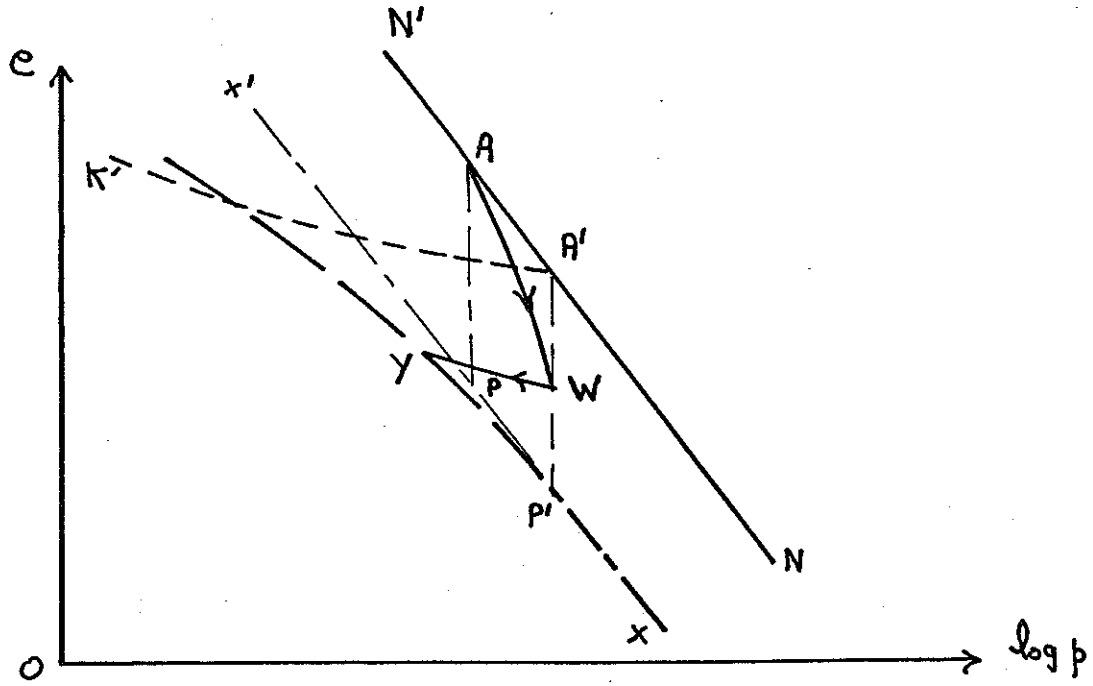

(b)

Fig. 5.5. The paths followed by specimens in Type 4 tests in (a) the (q,p) space and (b) the (e, log p) space.

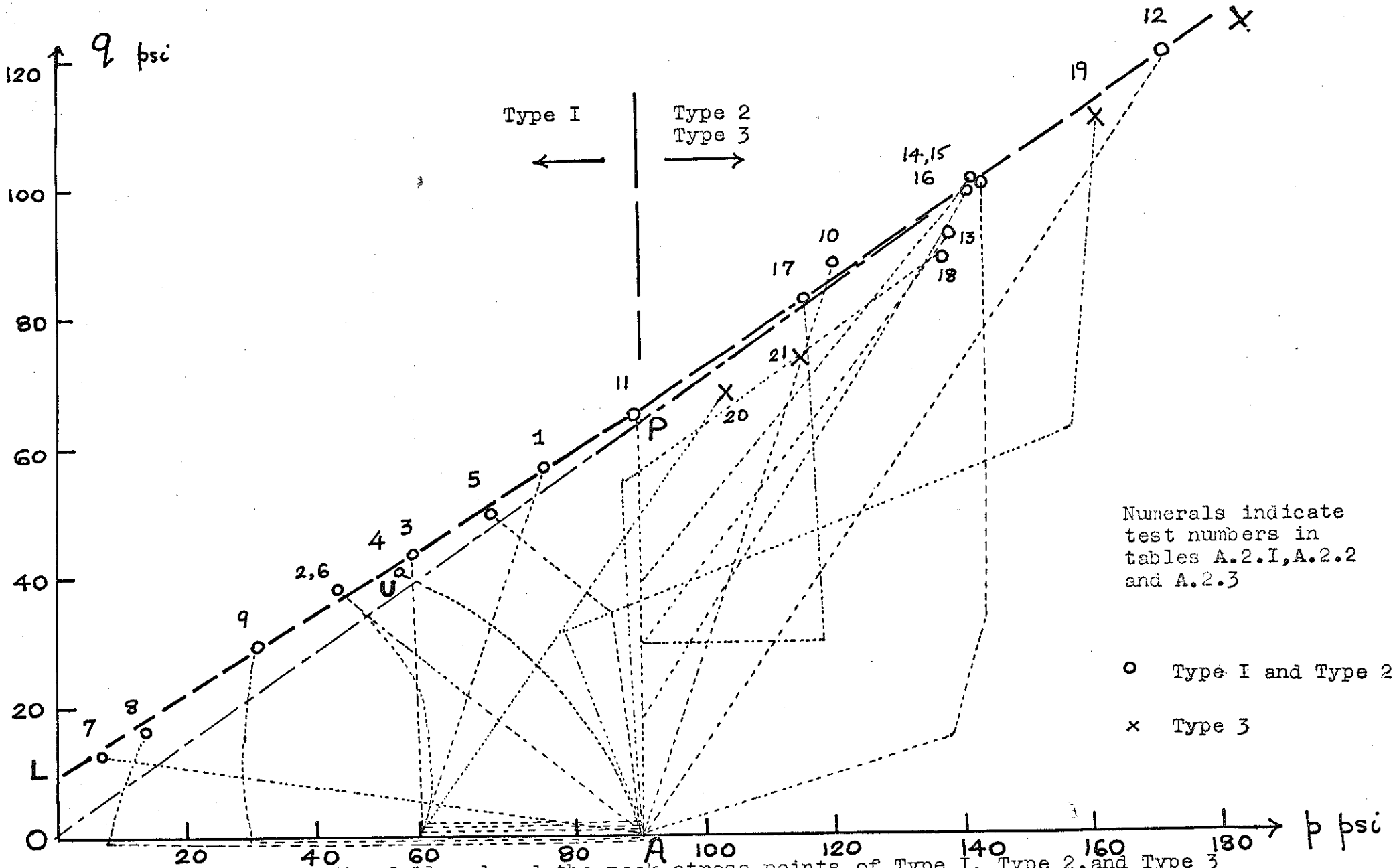

Fig. 5.6. The stress paths followed and the peak stress points of Type I, Type 2, and Type 3 tests of specimens sheared from an isotropic stress of 90 psi.

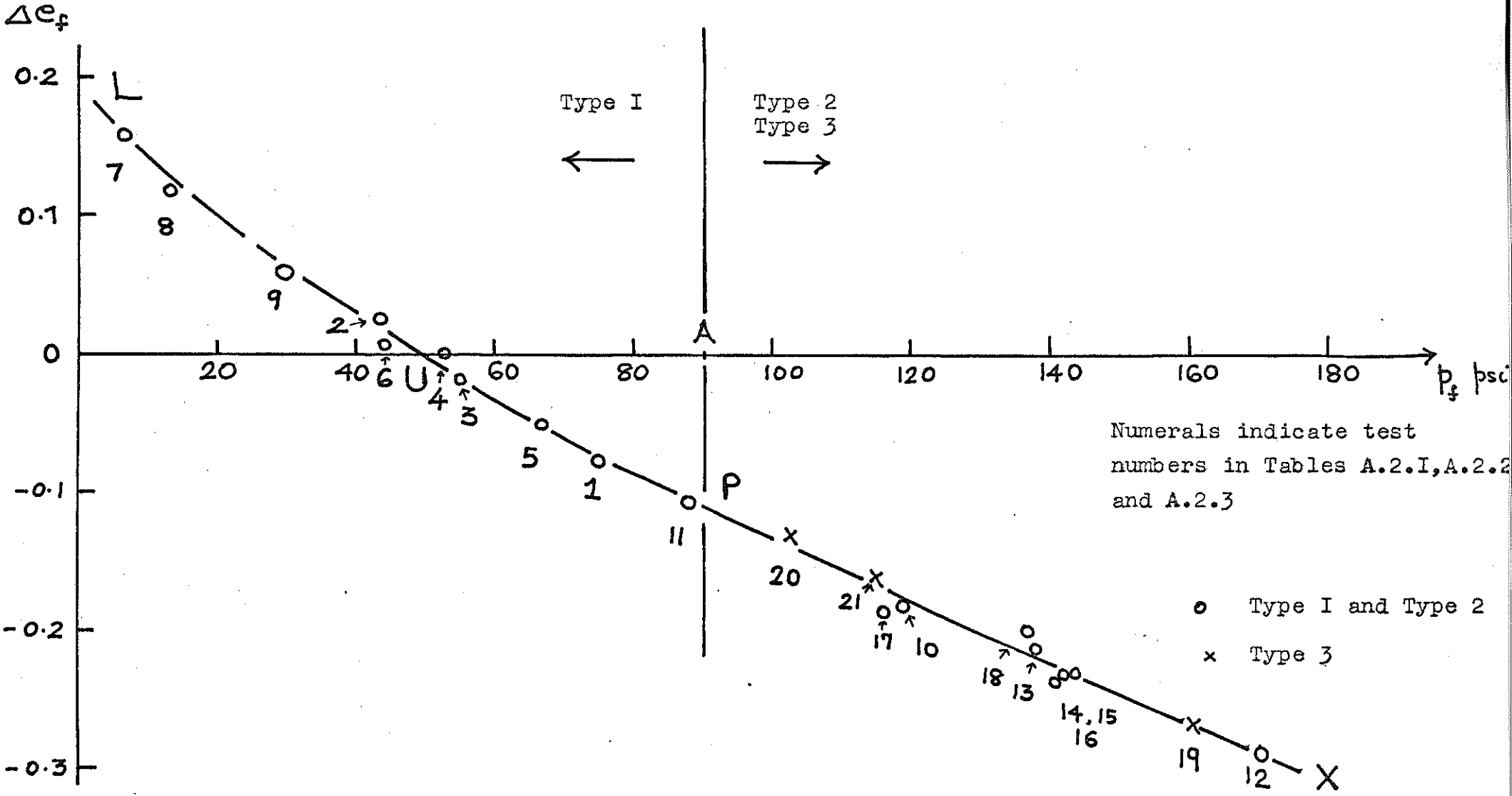

Fig. 5.7. The peak stress points in (Δe_f, p_f) space of specimens sheared along Type I, Type 2 and Type 3 stress paths from an isotropic stress of 90 psi.

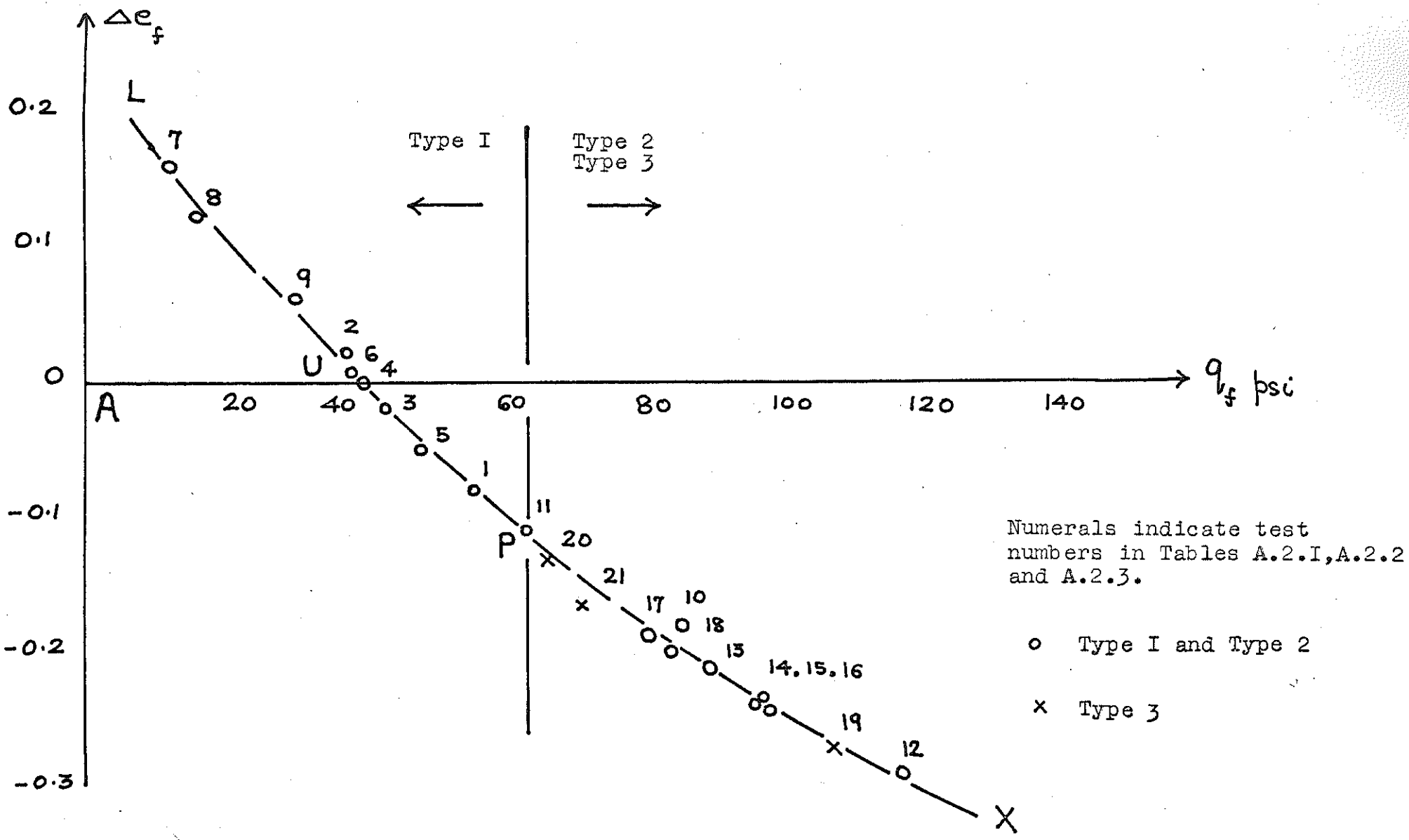

Fig. 5.8. The peak stress points in (Δe_f, q_f) space of specimens sheared along Type I, Type 2 Type 2 and type 3 stress paths from an isotropic stress of 90 psi.

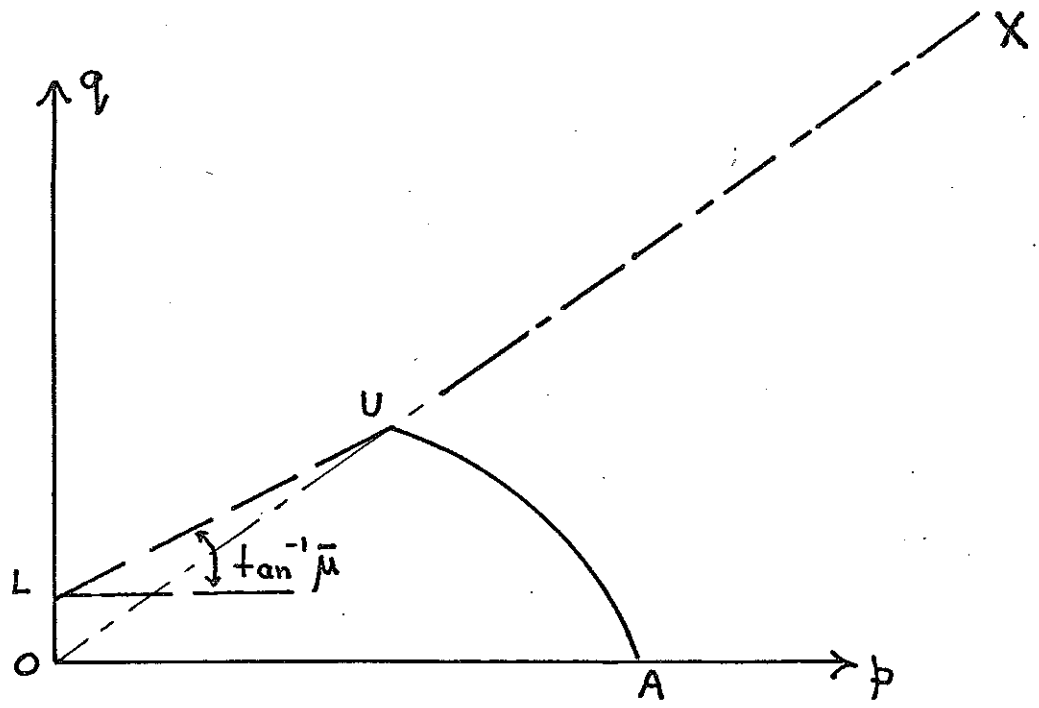

Fig. 5.9. The section of the Hvorslev surface in the constant voids ratio plane.

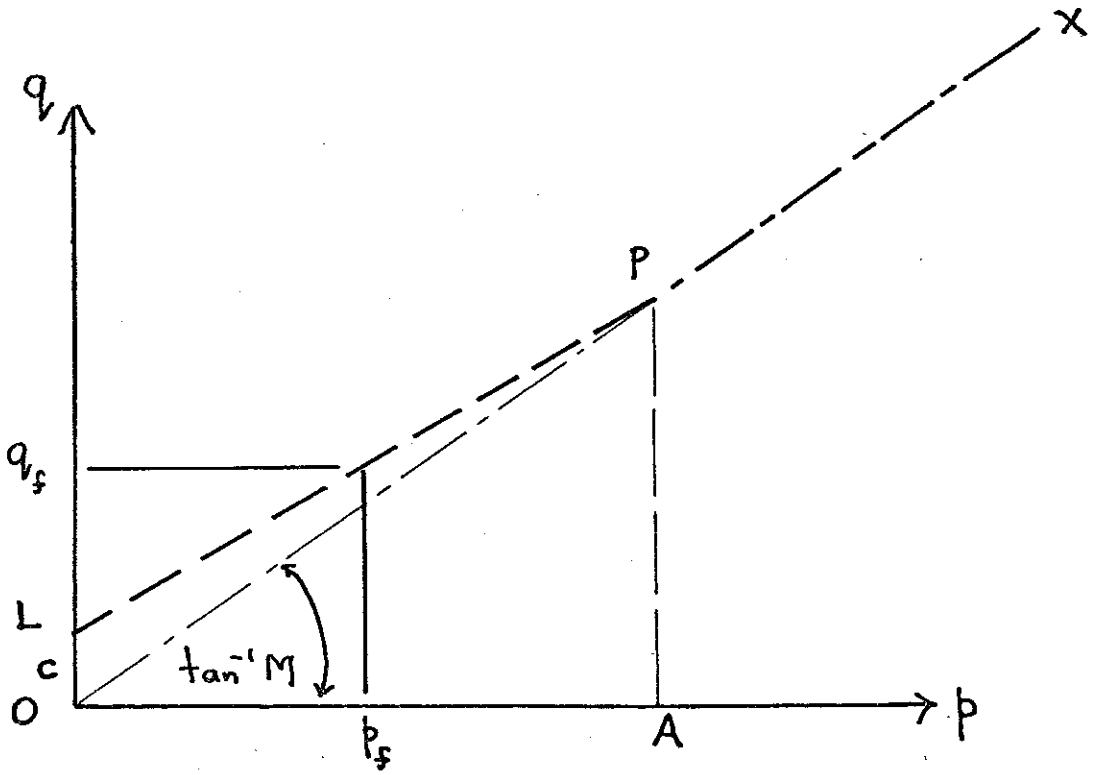

Fig. 5.10. The projection of the Author's failure surface in the (q,p) plane.

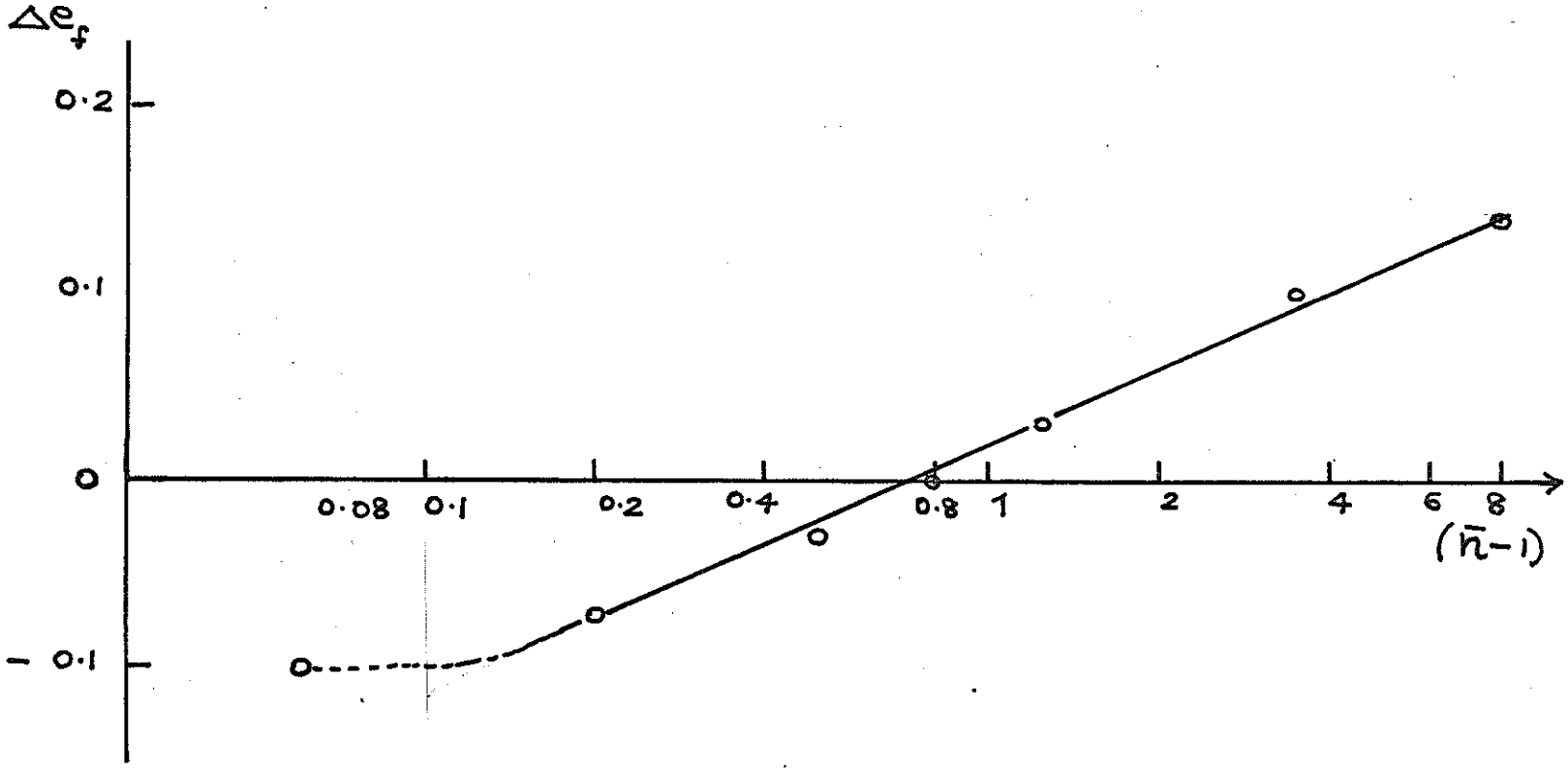

Fig. 5.II. The (Δe_f, log(n-I)) characteristic of all specimens sheared along Type I, Type 2 and Type 3 stress paths from an isotropic stress of 90 psi.

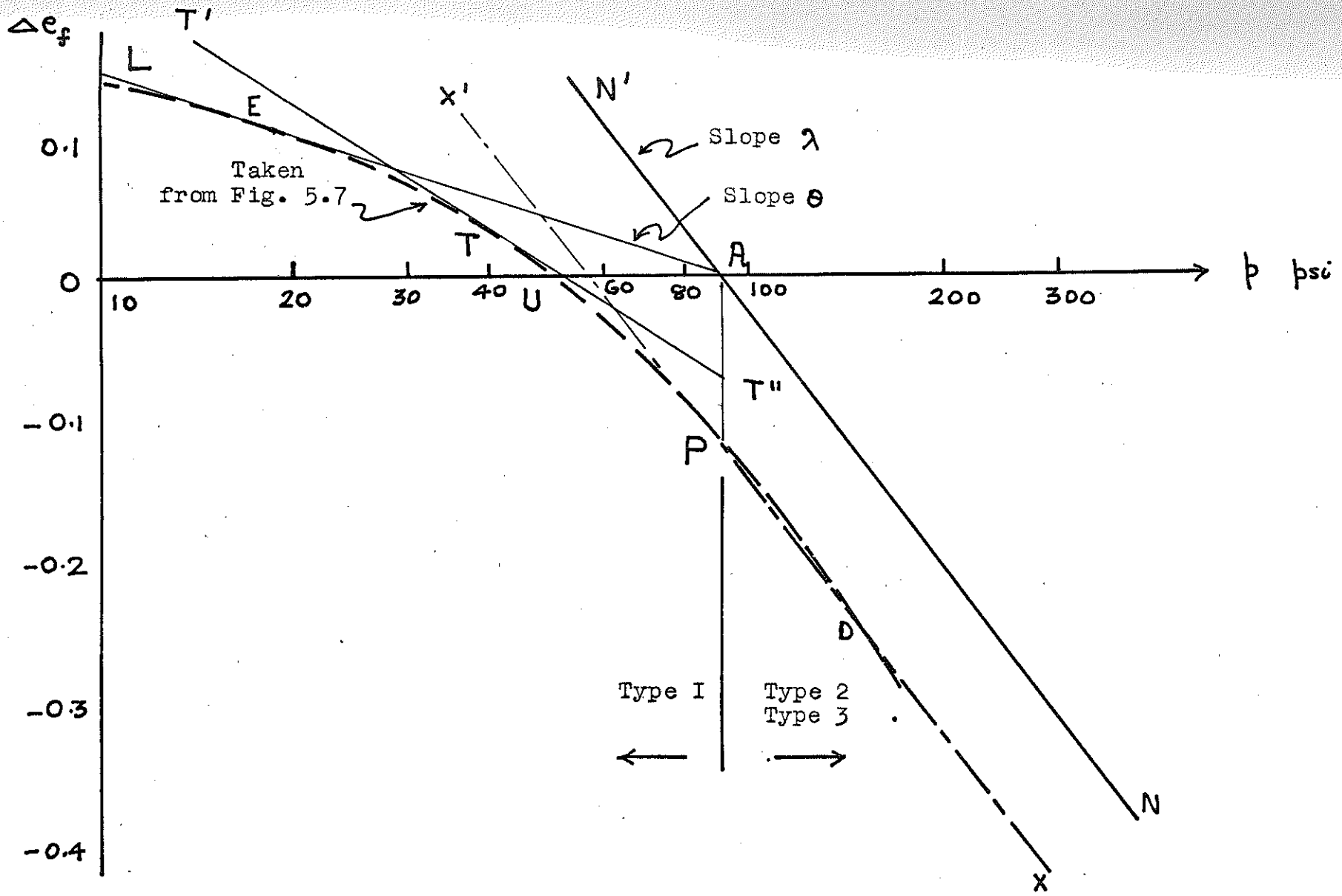

Fig. 5.I2. The (Δe_f, log p_f) characteristic for all specimens sheared along stress paths of Type I, Type 2, and Type 3 from an isotropic stress of 90 psi.

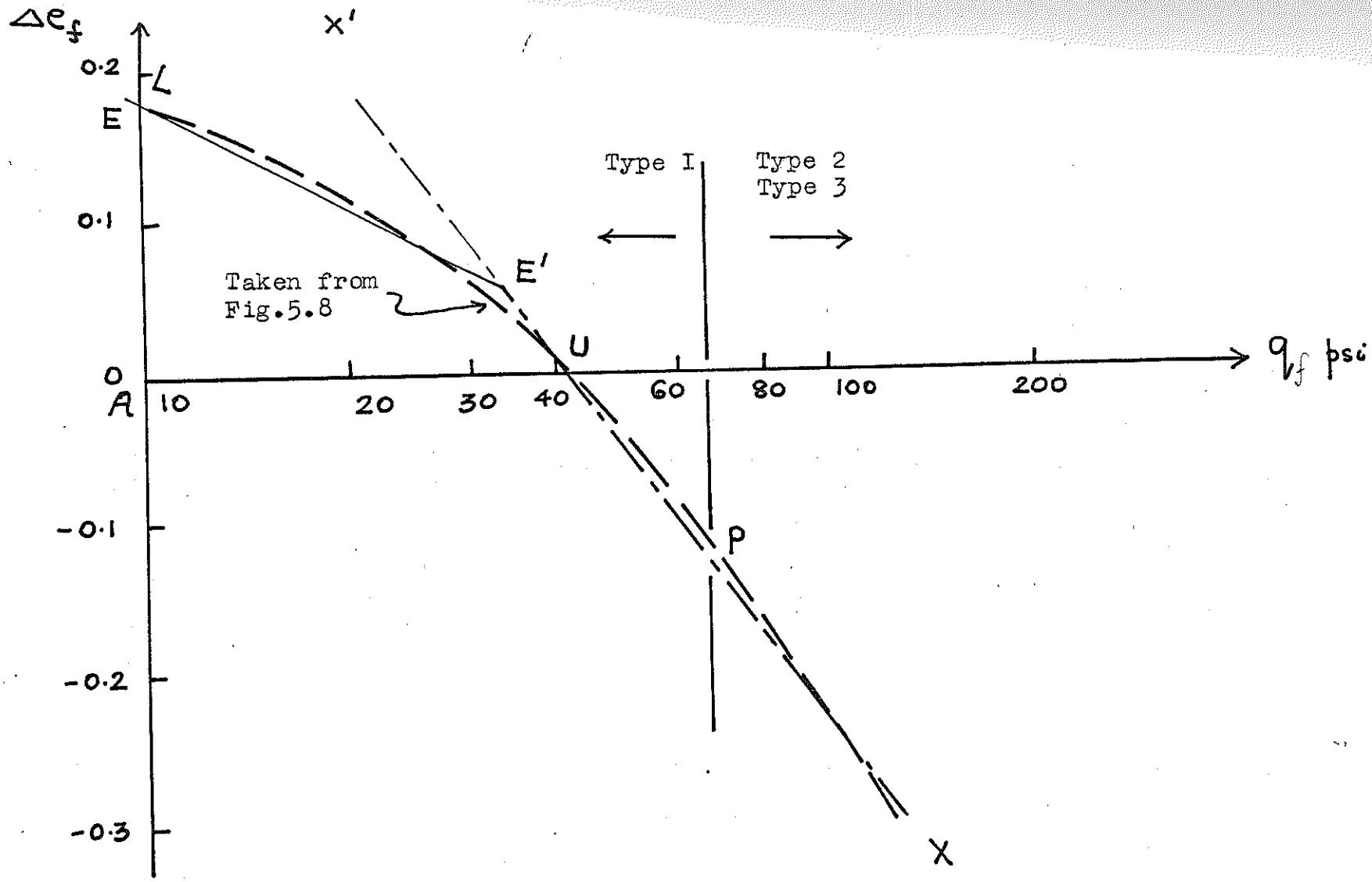

Fig. 5.13. The (Δe_f , log (q_f)) characteristic for all specimens sheared along stress paths of Type I, Type 2 and Type 3 from an isotropic stress of 90 psi.

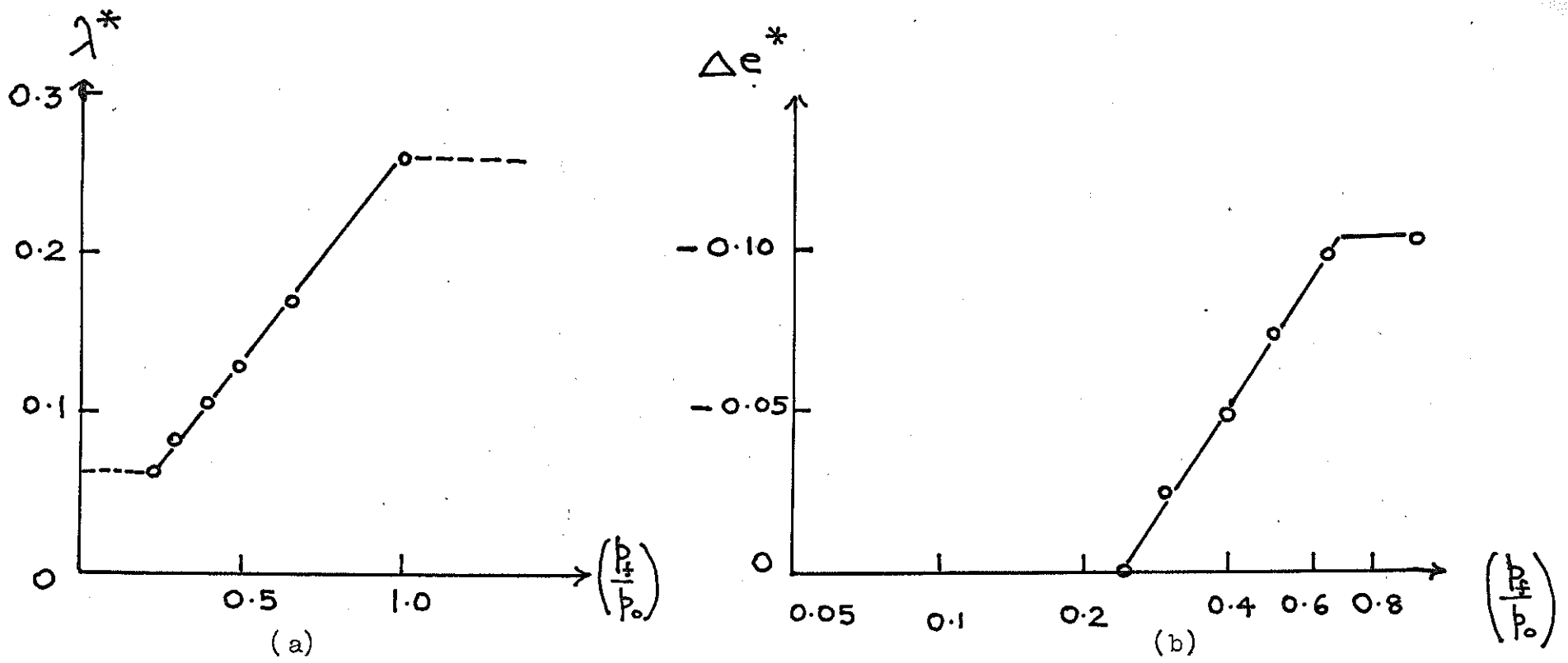

Fig. 5. I4 . (a) The (λ^*, P_f/p_o) and (b) the (Δe^*, $\log(p_f/p_o)$) characteristics for all specimens sheared along stress paths of Type I, Type 2 and Type 3 from an isotropic stress of 90 psi.

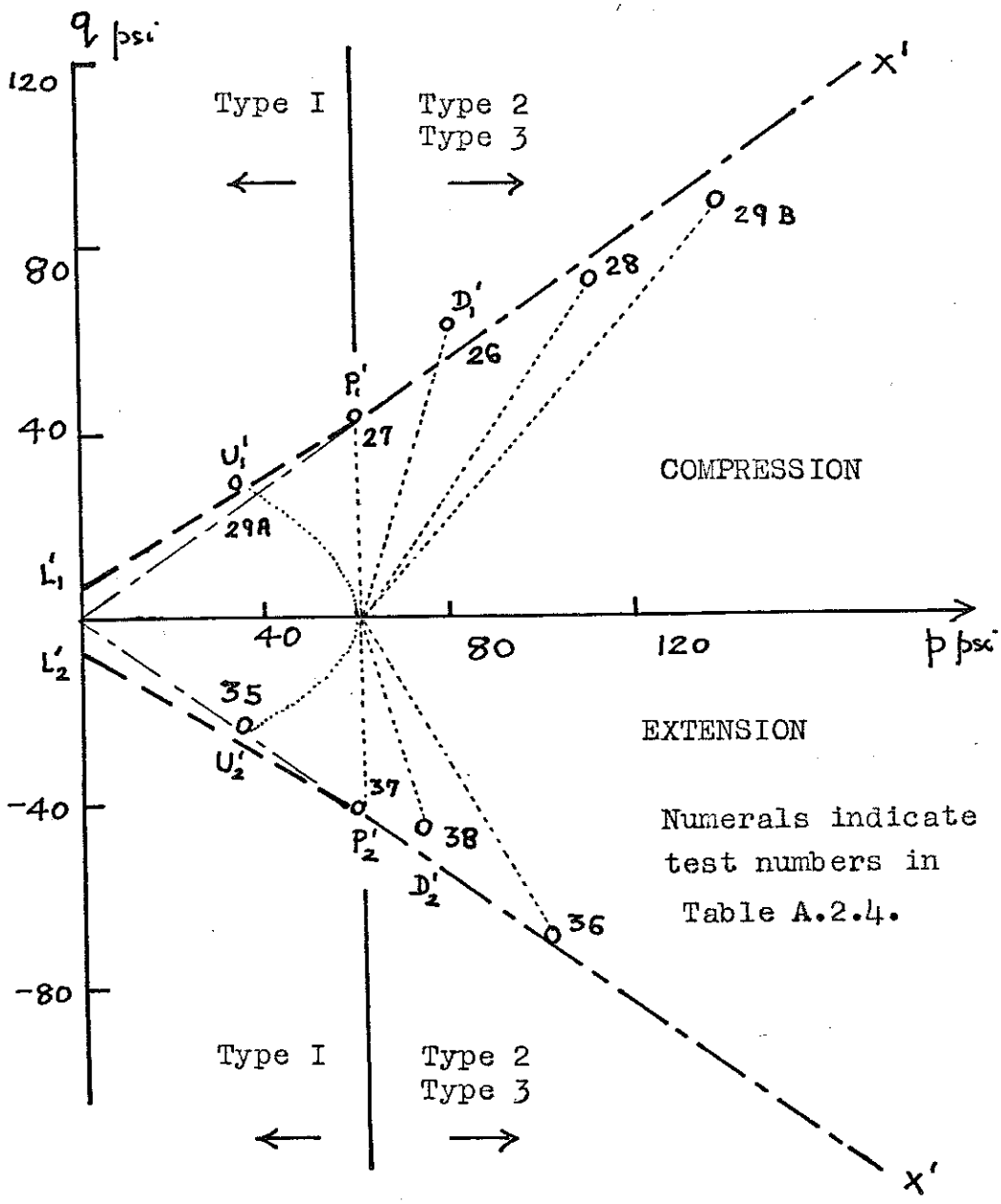

Fig. 5.15. The stress paths followed and the peak stress points of all specimens sheared from an isotropic stress of 60 psi.

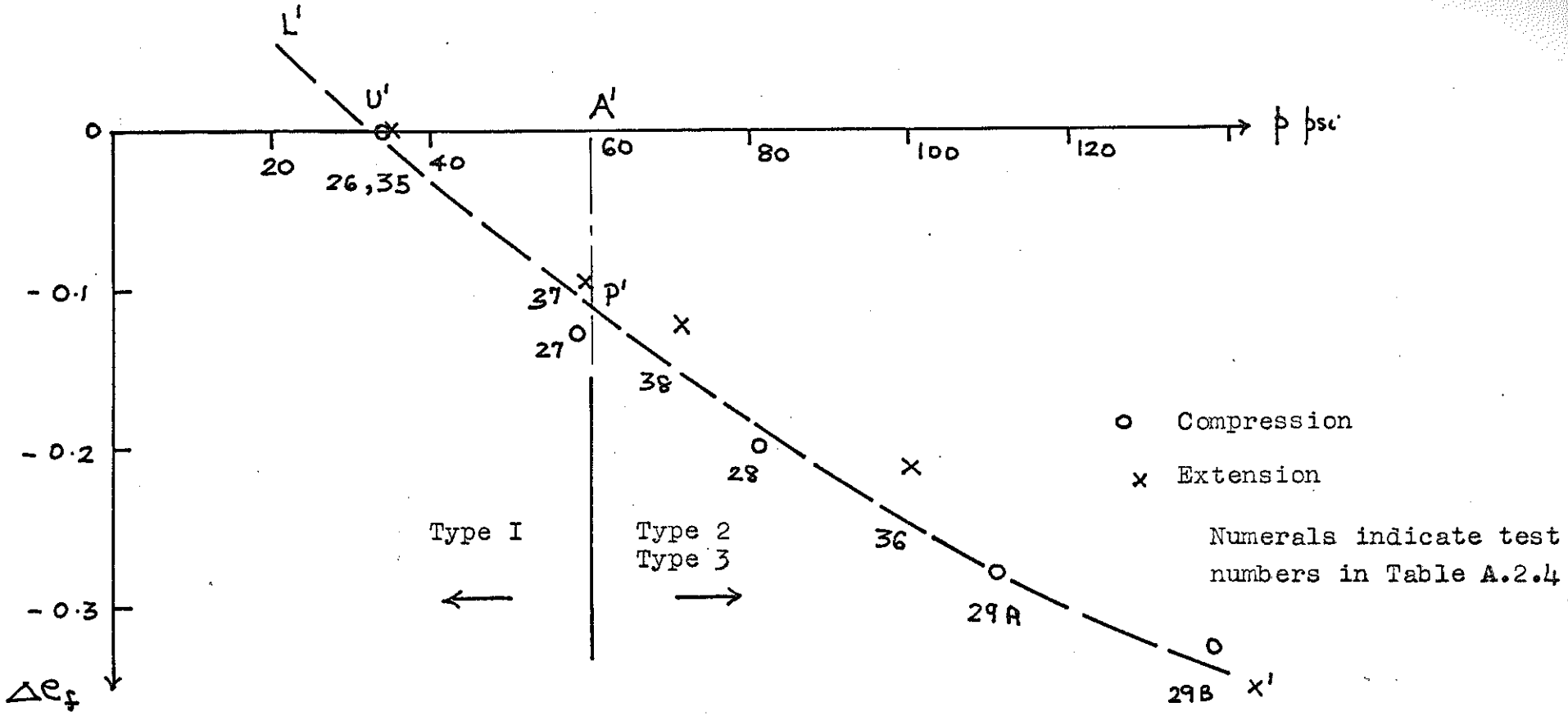

F ig. 5.I6. The (Δe_f, p_f) characteristic of all specimens sheared from an isotropic stress of 60 psi.

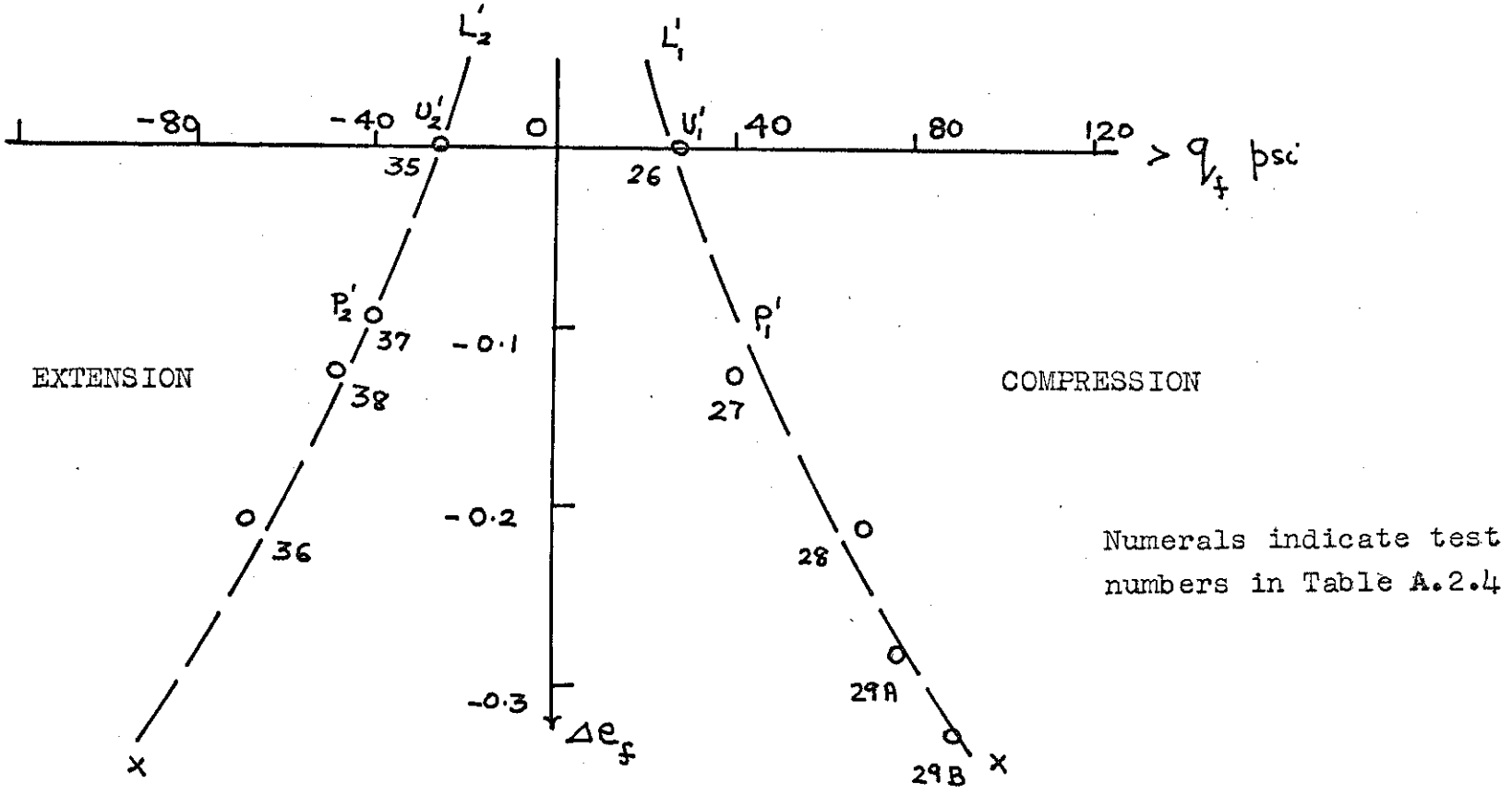

Fig. 5.17. The (Δe_f, q_f) characteristics of all specimens sheared from an isotropic stress of 60 psi.

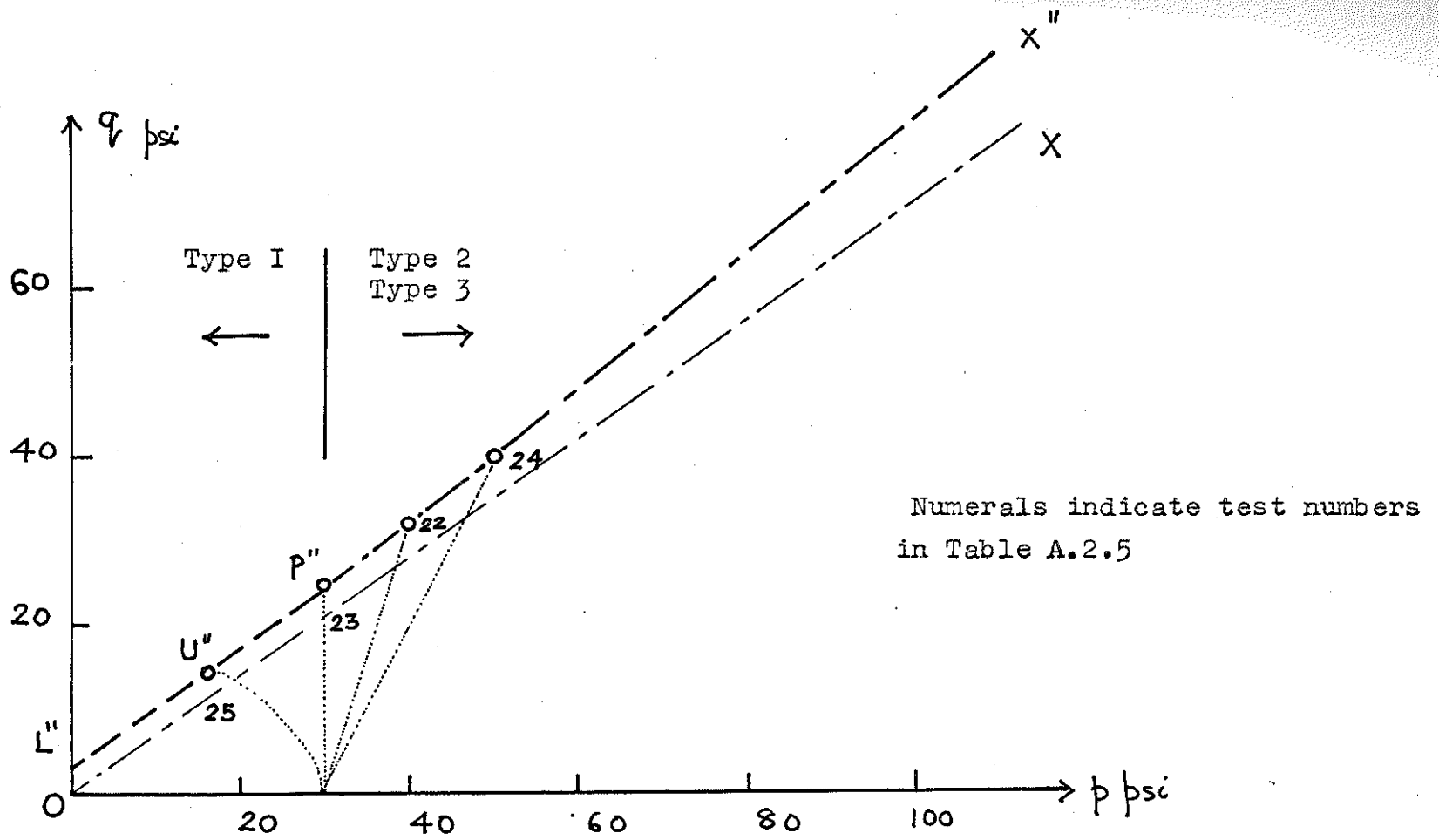

Fig. 5.I8. The stress paths followed and the peak stress points of all specimens sheared from an isotropic stress of 30 psi.

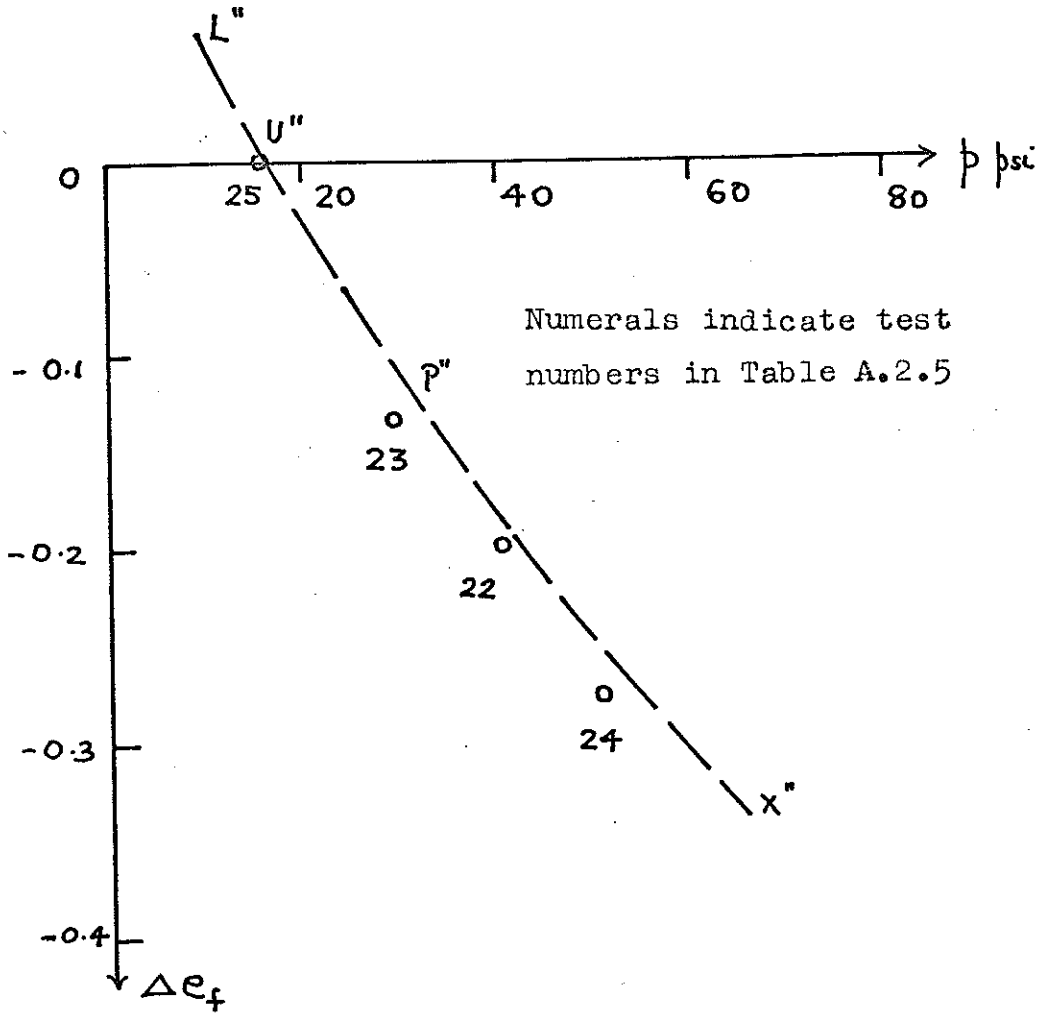

Fig.5.I9. The (Δe_f, p_f) characteristic of all specimens sheared from an isotropic stress of 30 psi.

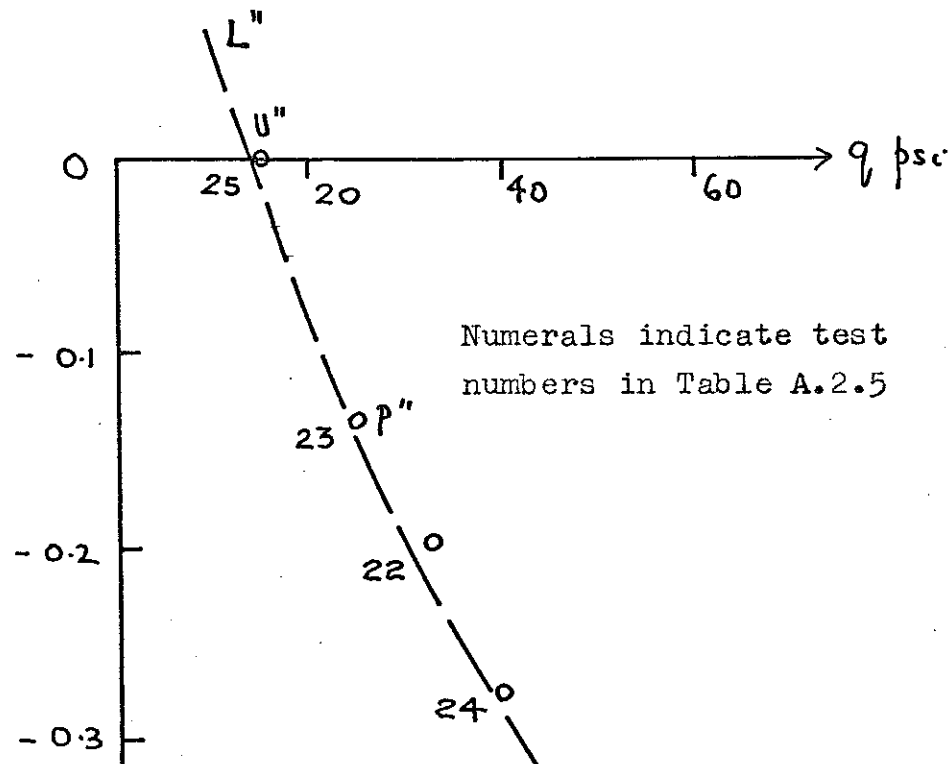

Fig. 5.20. The $(\Delta e_f, q_f)$ characteristic of all specimens sheared from an isotropic stress of 30 psi.

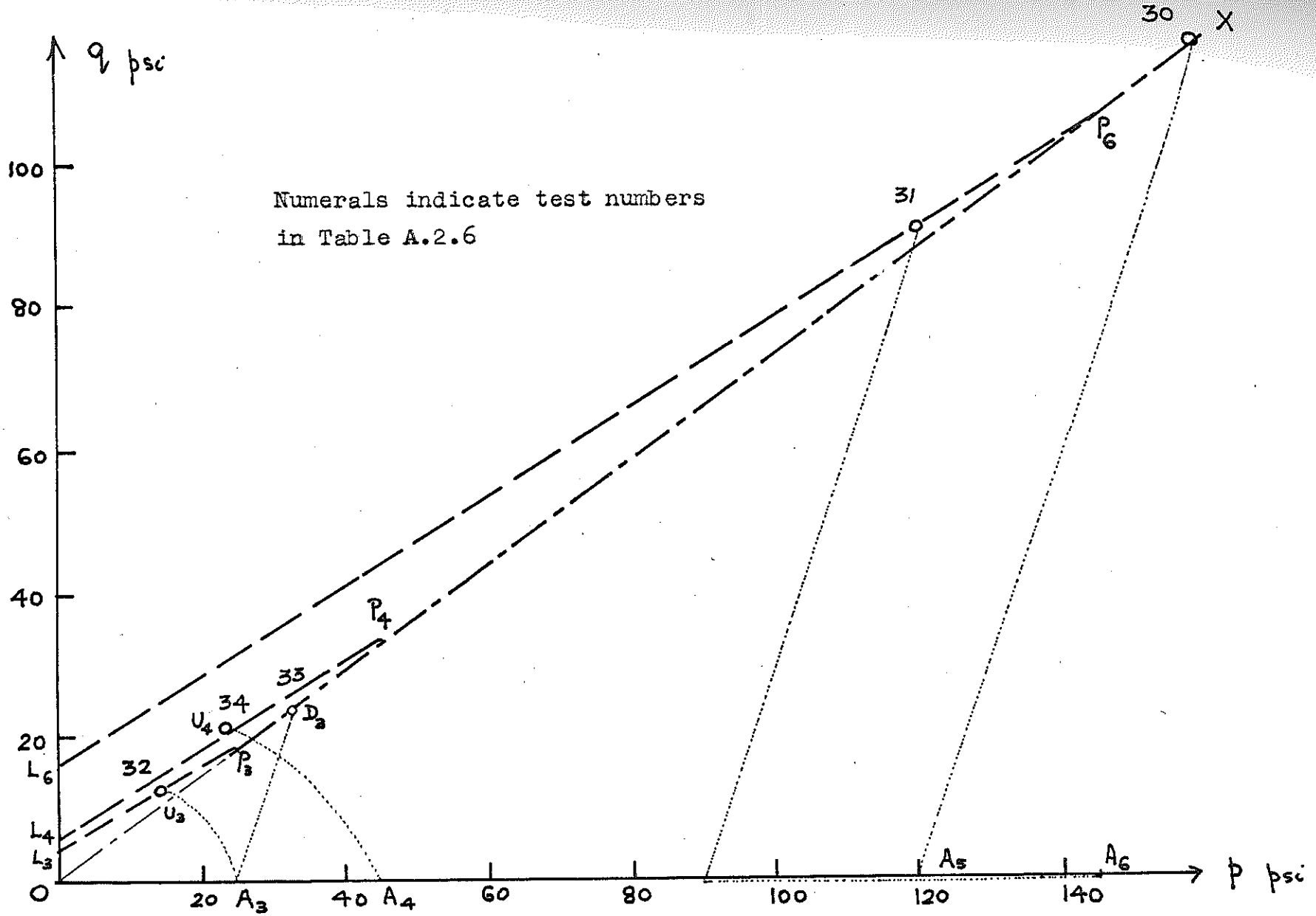

Fig. 5.2I. The stress paths followed and the peak stress points of specimens sheared from miscellaneous isotropic stress conditions.

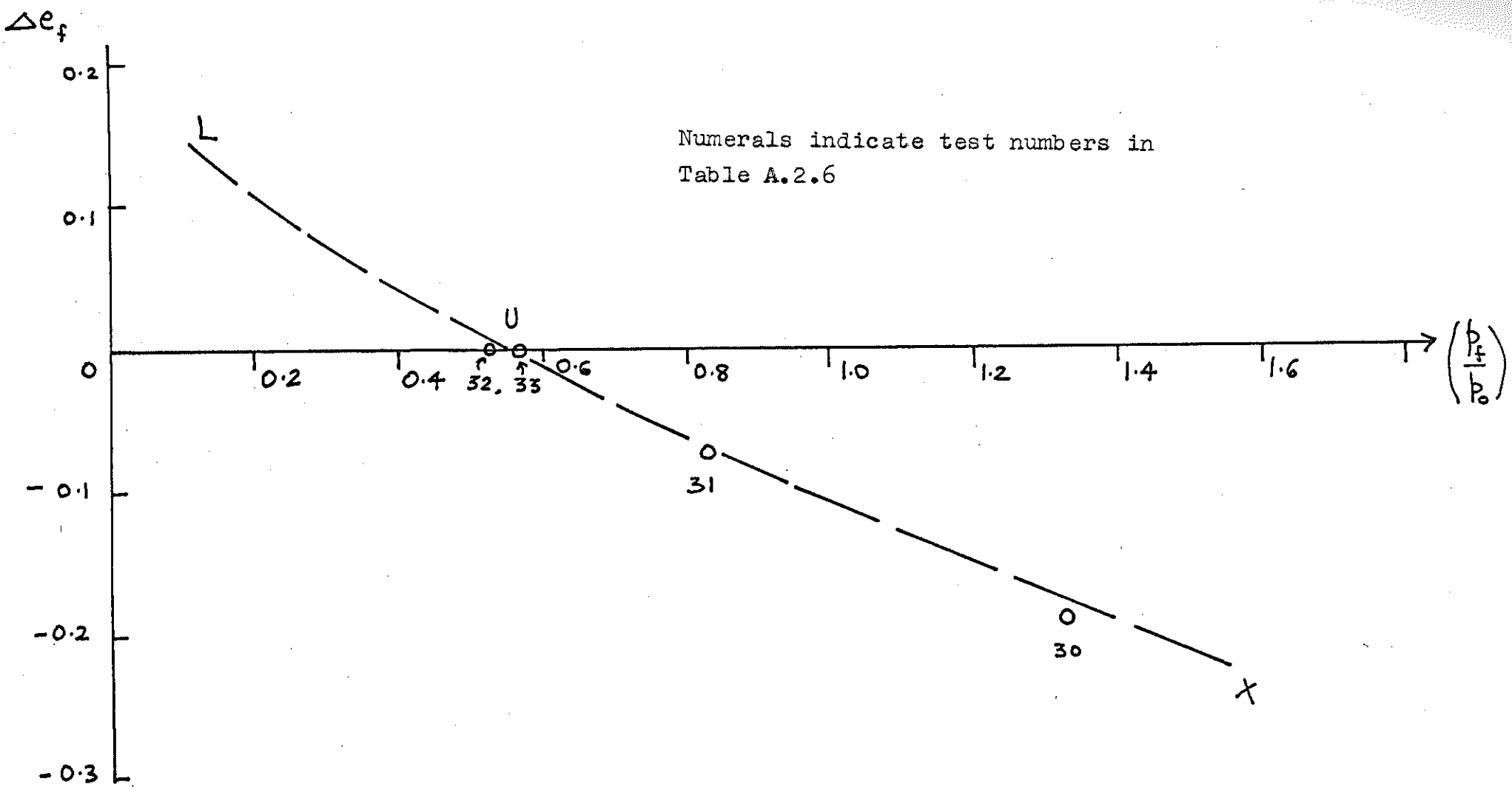

Fig. 5.22. The (Δe, p_f/p_o) characteristics of specimens sheared from miscellaneous isotropic stress conditions.

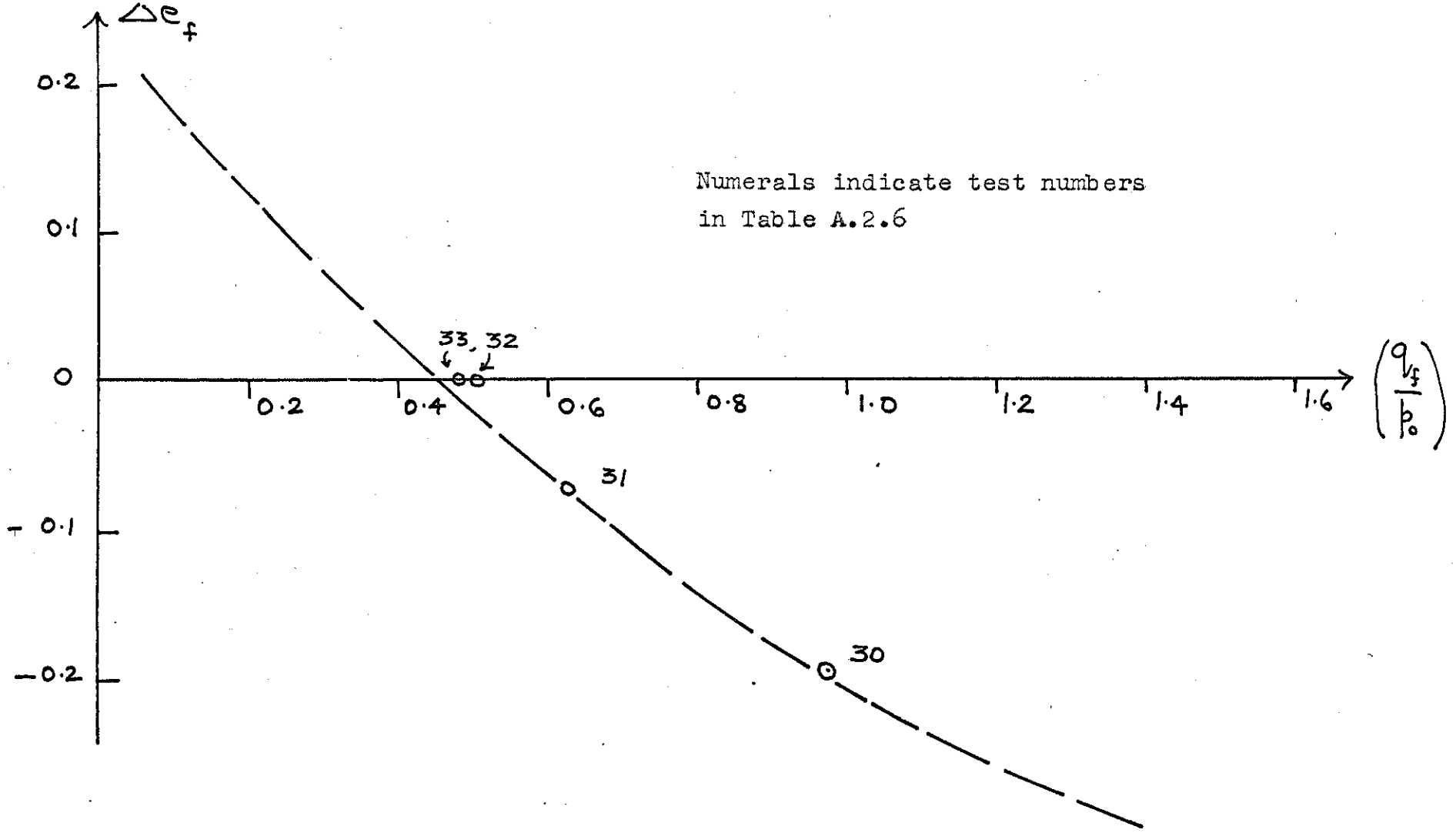

Fig. 5.23. The (Δe, q_f/p_o) characteristics of specimens sheared from miscellaneous isotropic stress conditions.

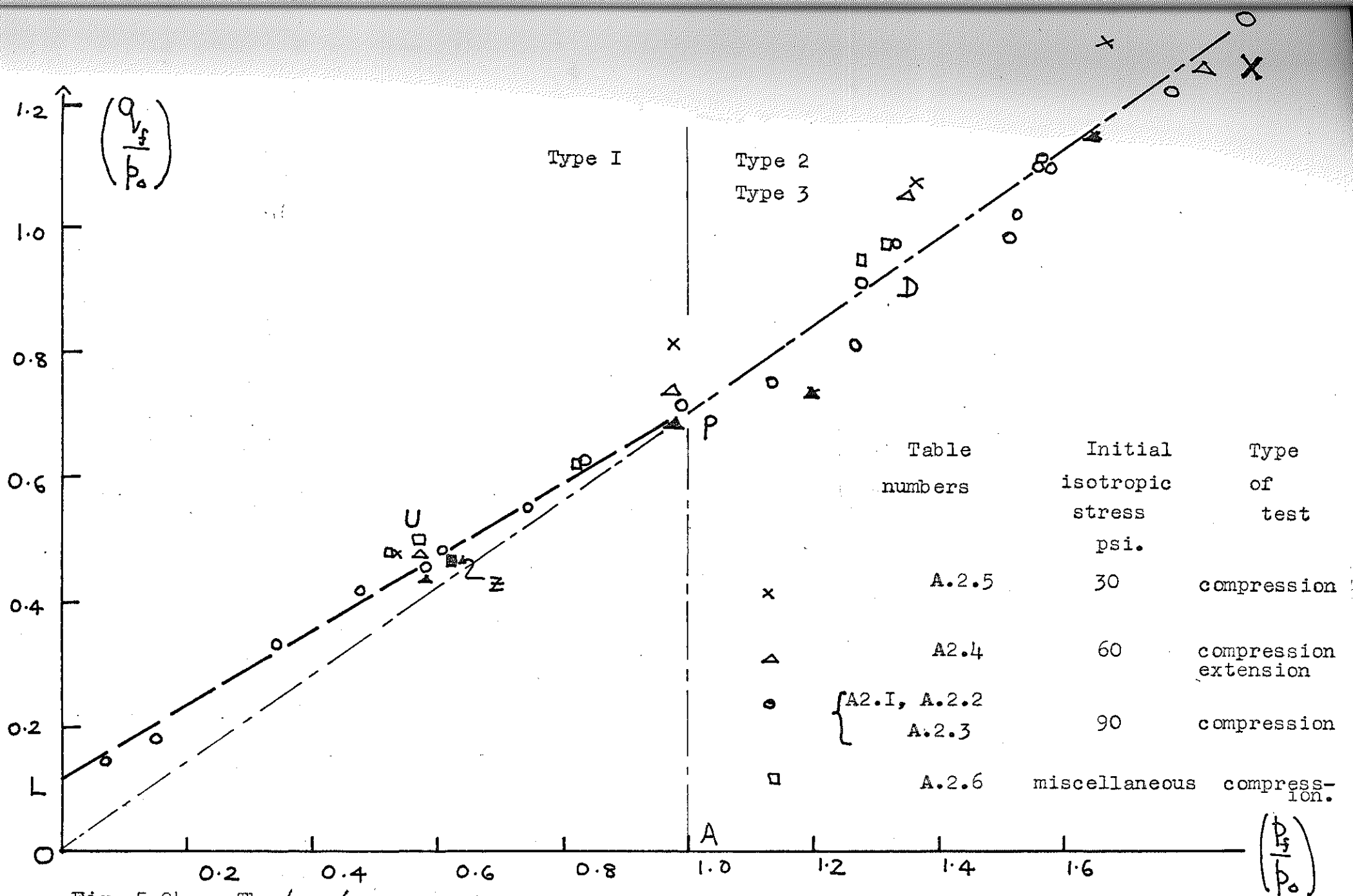

Fig. 5.24. The (q_f/p_o, p_f/p_o) characteristics of all specimens sheared along Type I, Type 2 and Type 3 test paths.

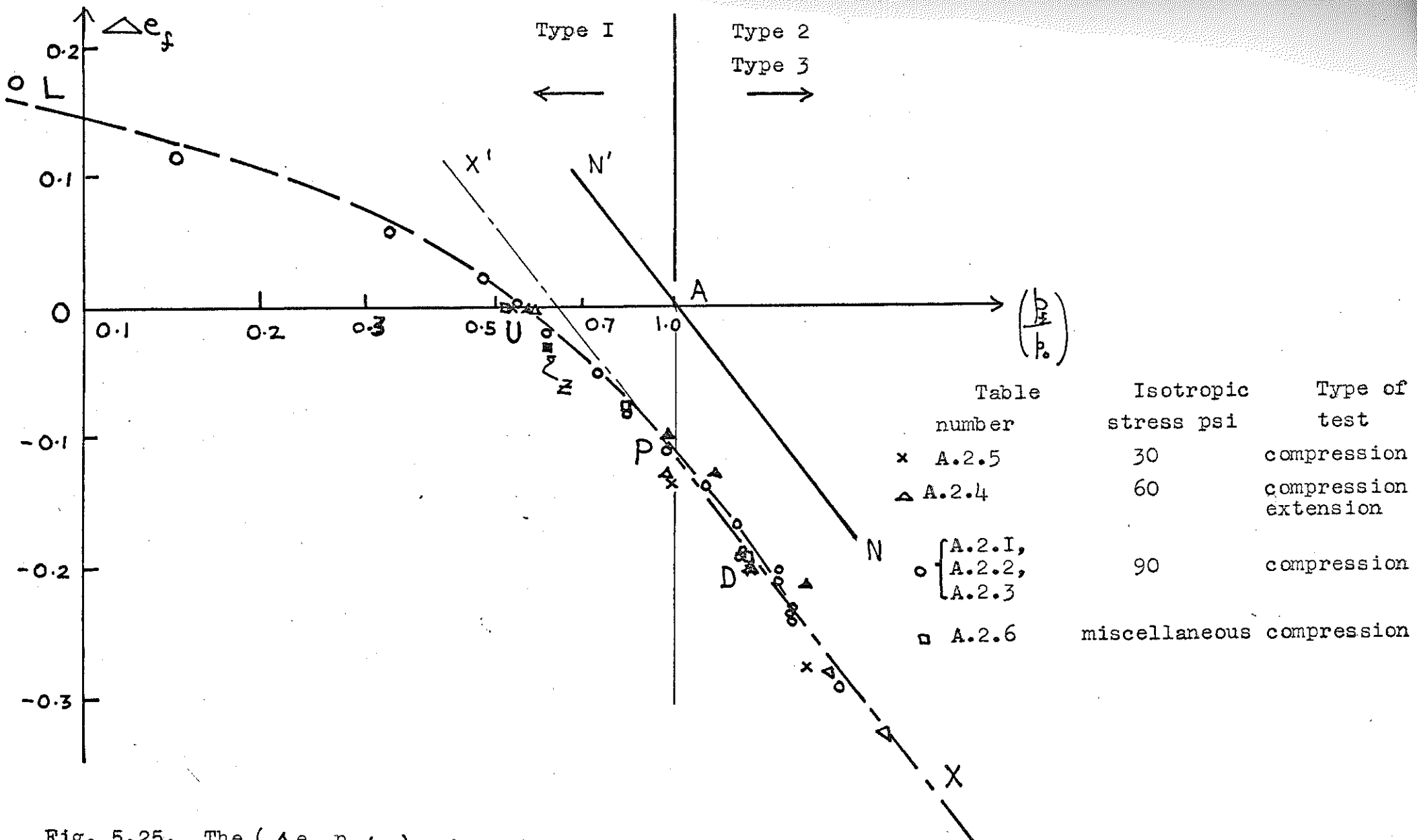

	Table number	Isotropic stress psi	Type of test
×	A.2.5	30	compression
△	A.2.4	60	compression extension
○	A.2.1, A.2.2, A.2.3	90	compression
□	A.2.6	miscellaneous	compression

Fig. 5.25. The (Δe_f, p_f/p_o) characteristics of all specimens sheared along Type I, Type 2, Type 3 test paths.

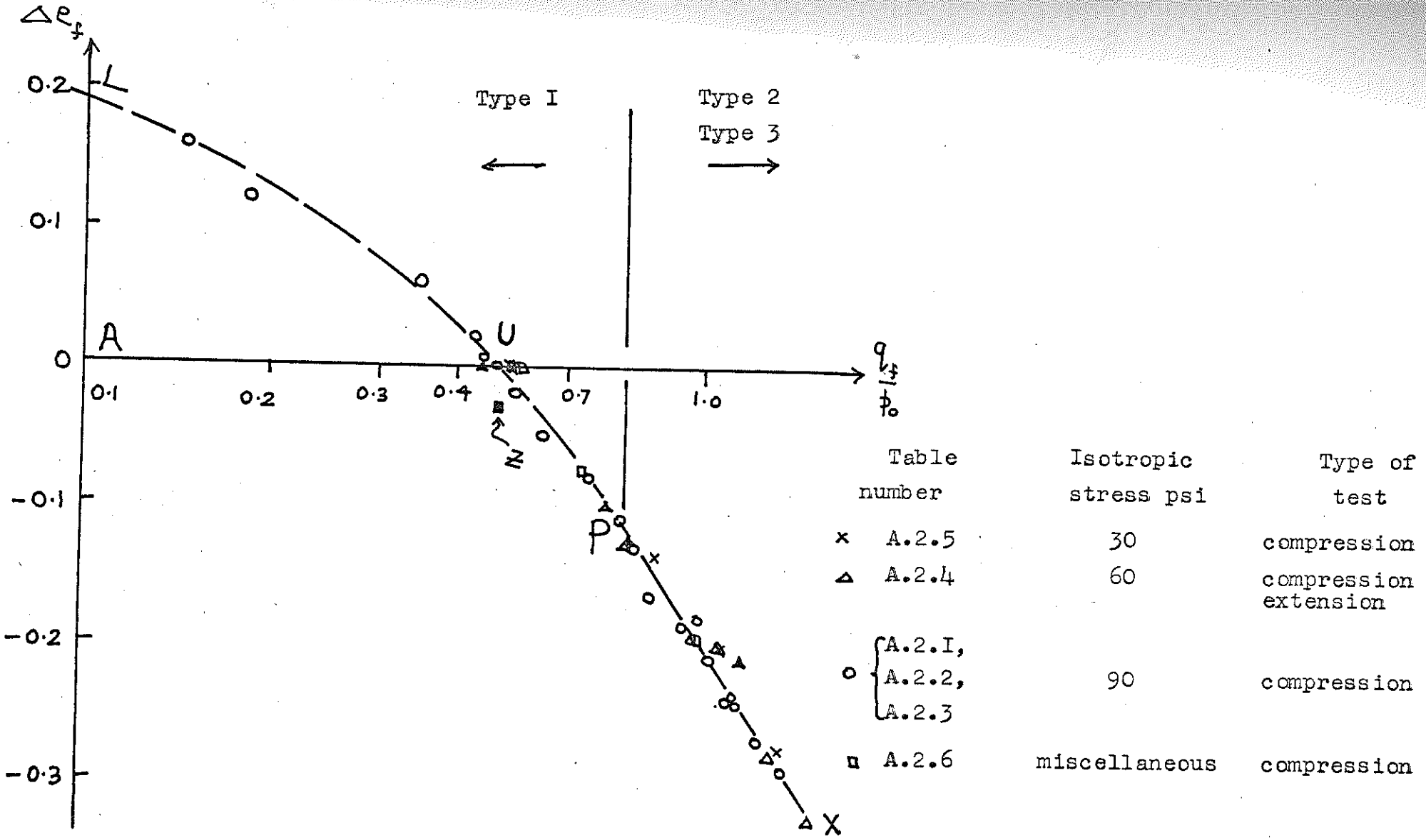

	Table number	Isotropic stress psi	Type of test
×	A.2.5	30	compression
△	A.2.4	60	compression extension
○	A.2.I, A.2.2, A.2.3	90	compression
▫	A.2.6	miscellaneous	compression

Fig. 5.26. The (Δe_f, q_f/p_o) characteristics of all specimens sheared along TypeI, Type 2 and Type 3 stress paths.

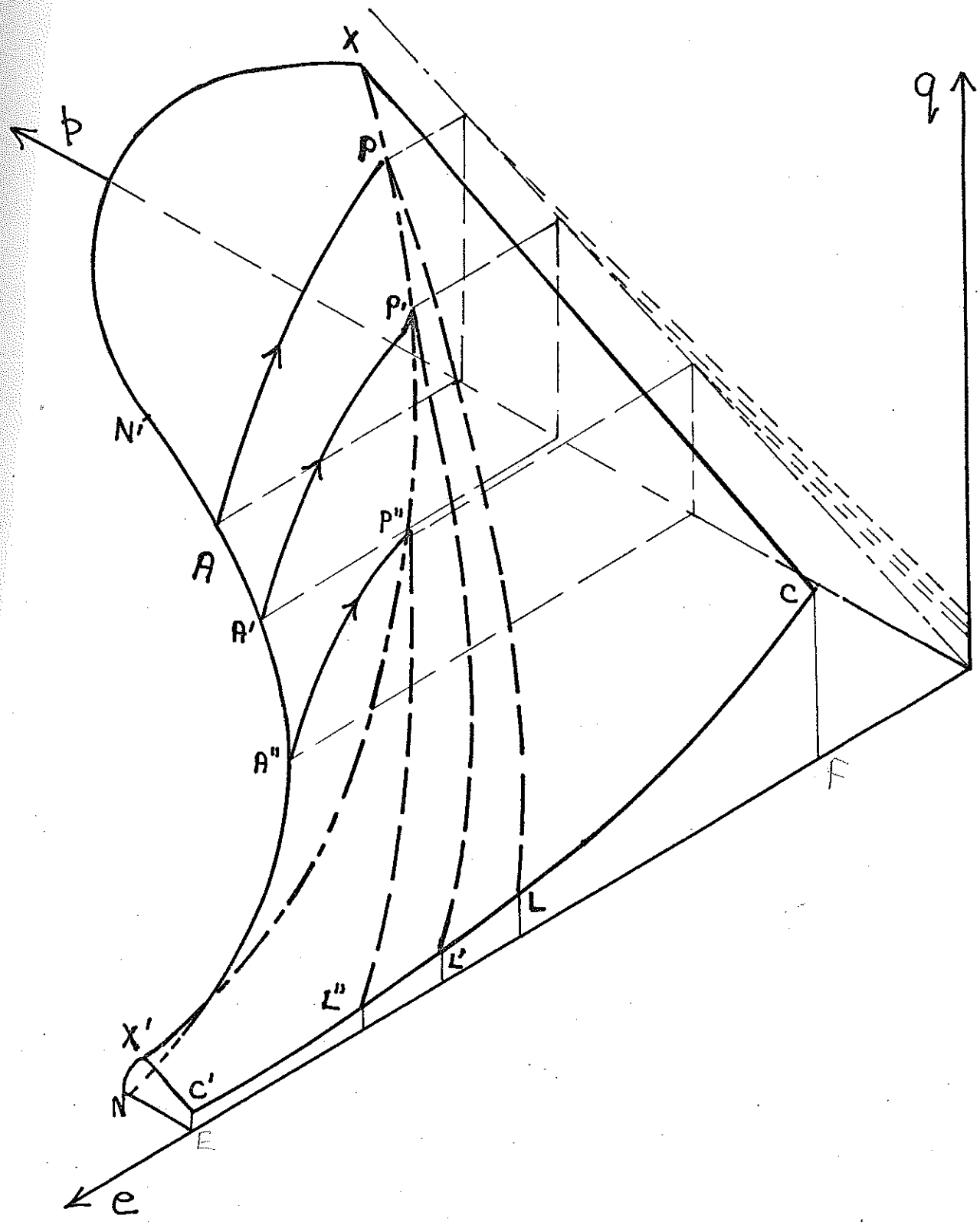

Fig. 5.27. The critical state line and the Hvorslev surface in the (p,q,e) space.

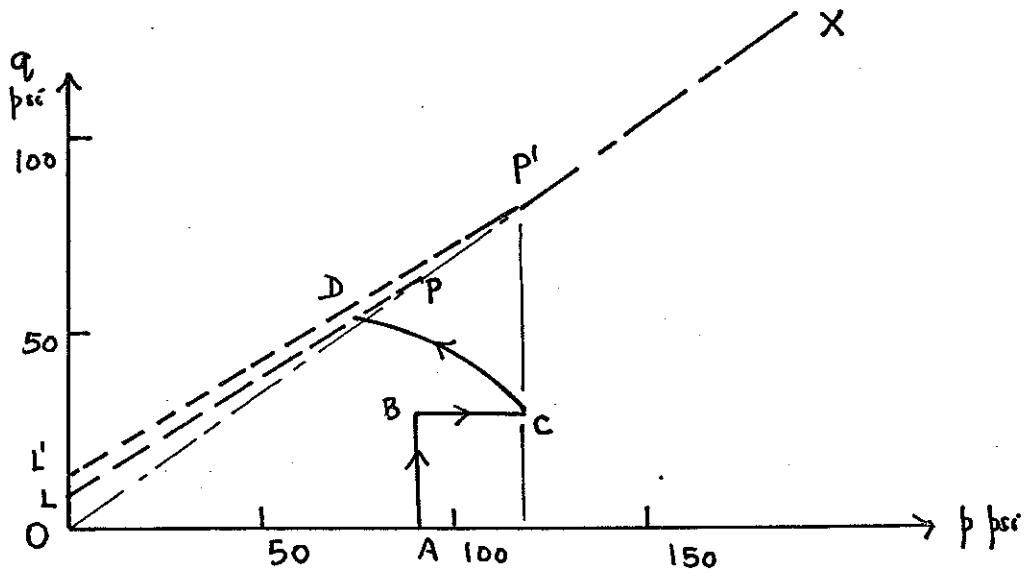

Fig. 5.27 (a). The stress path followed by specimen T_{I2} in (q,p) space.

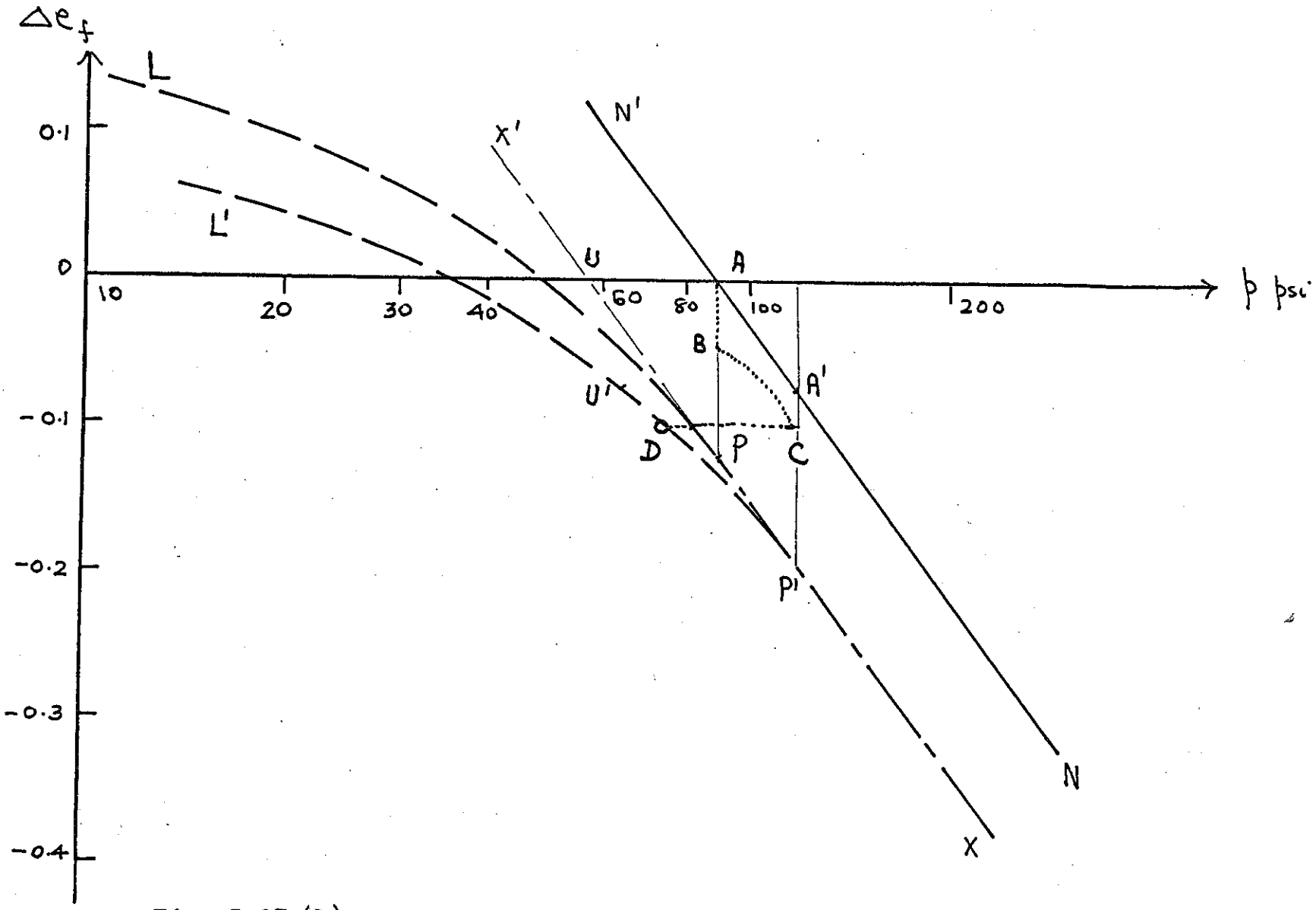

Fig. 5.27 (b). The peak stress point of specimen T_{I2} and the associated peak stress envelpos.

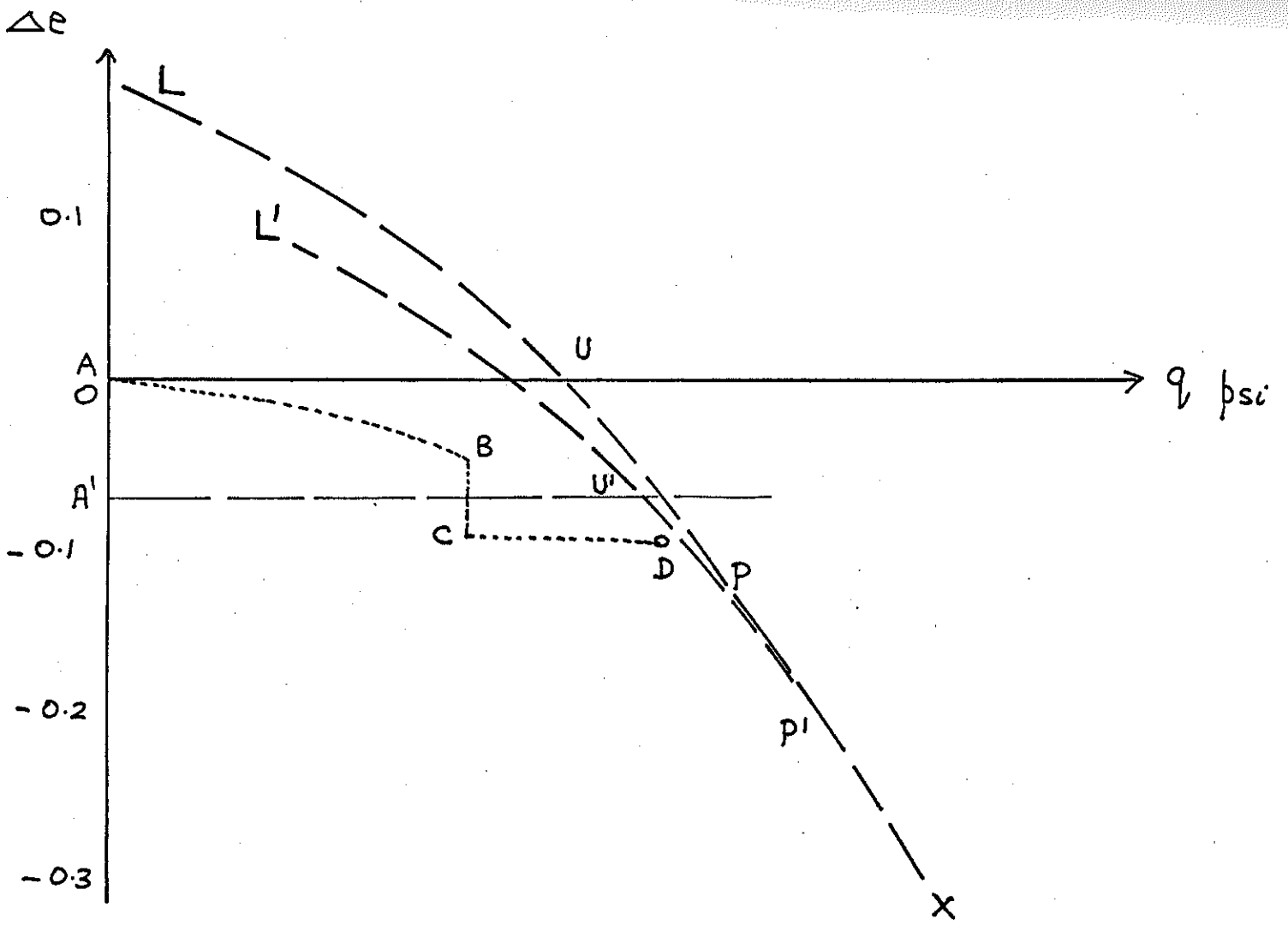

Fig. 5.27 (c). The peak stress point of specimen T_{I2} and the associated peak stress envelpos in (Δe, q) space.

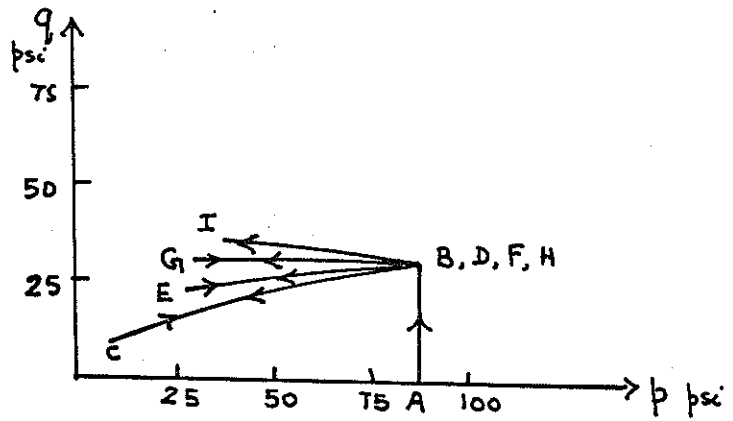

(a) The path followed by specimen T_{I7}

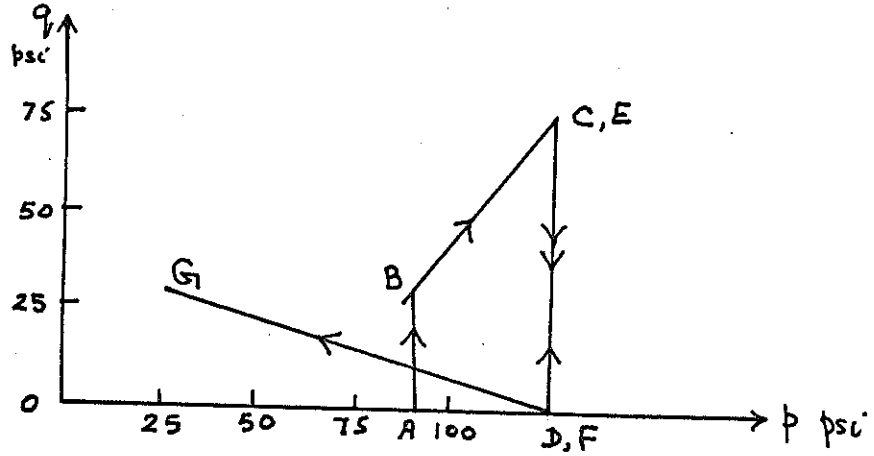

(b) The path followed by specimen BR.

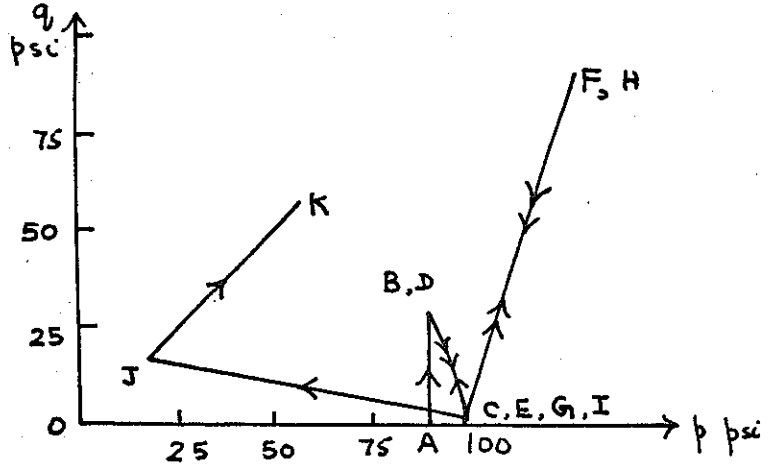

(c) The path followed by specimen BO

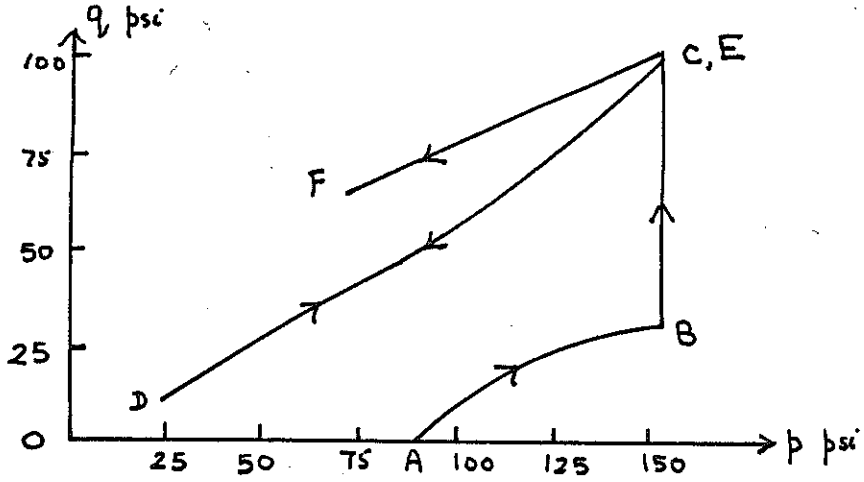

(d) The path followed by specimen BS.

Fig. 5.28. The stress paths followed by specimens T_{I7}, BR, BO and BS.

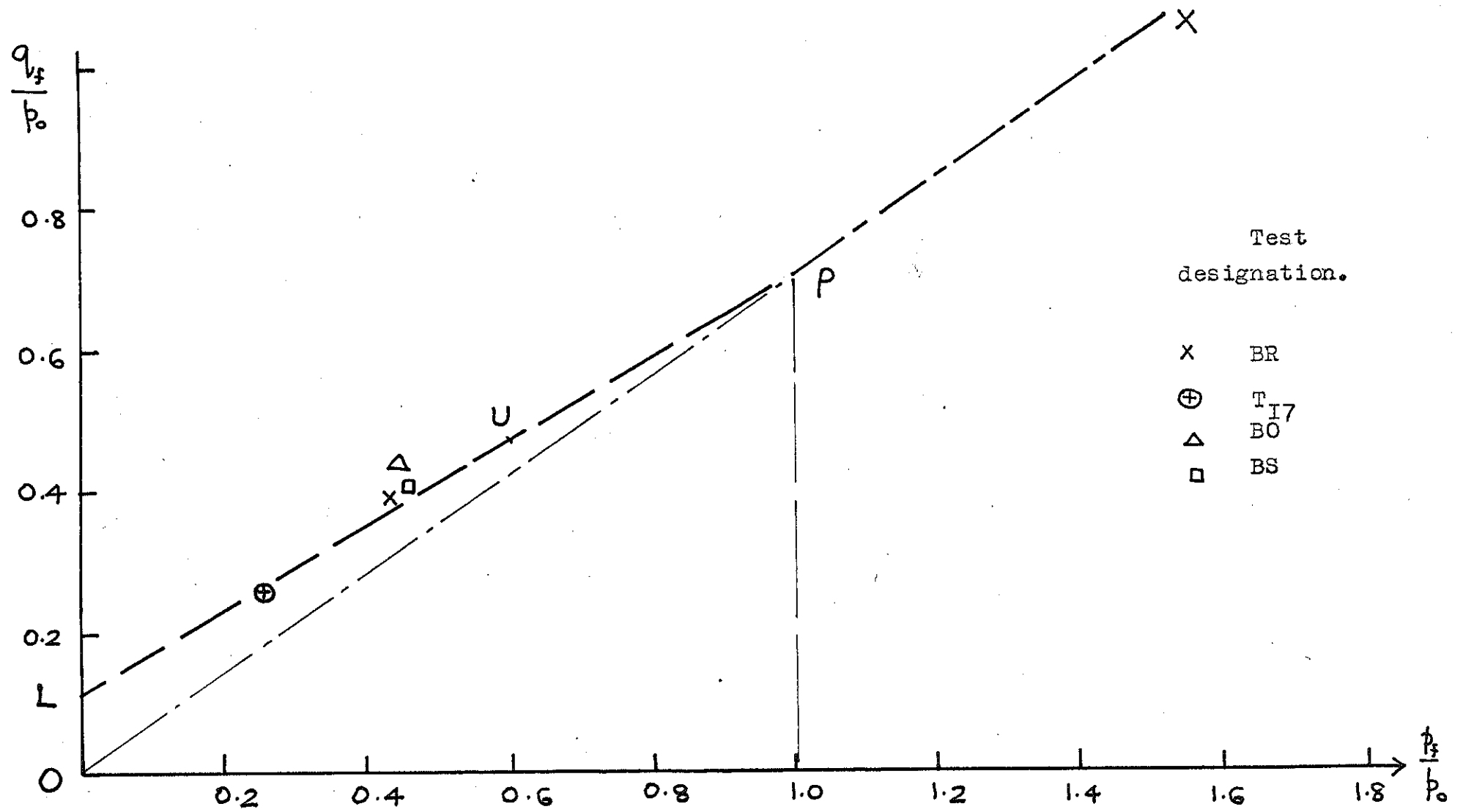

Fig. 5.29. The (q_f/p_o , p_f/p_o) characteristics of specimens T_{I7}, BR, BO and BS.

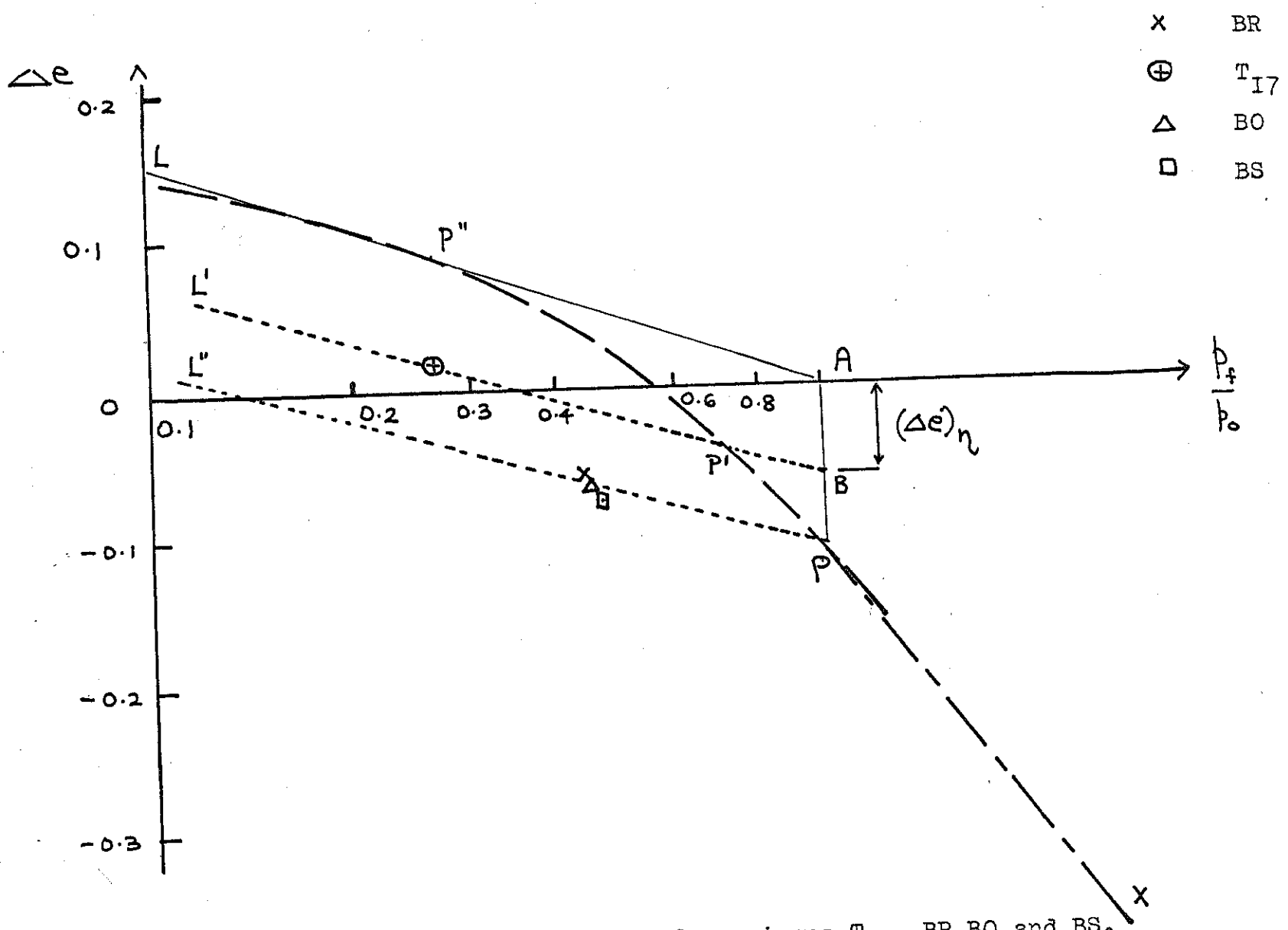

Fig. 5.30. The (e, p_f/p_o) characteristics of specimens T_{I7}, BR, BO and BS.

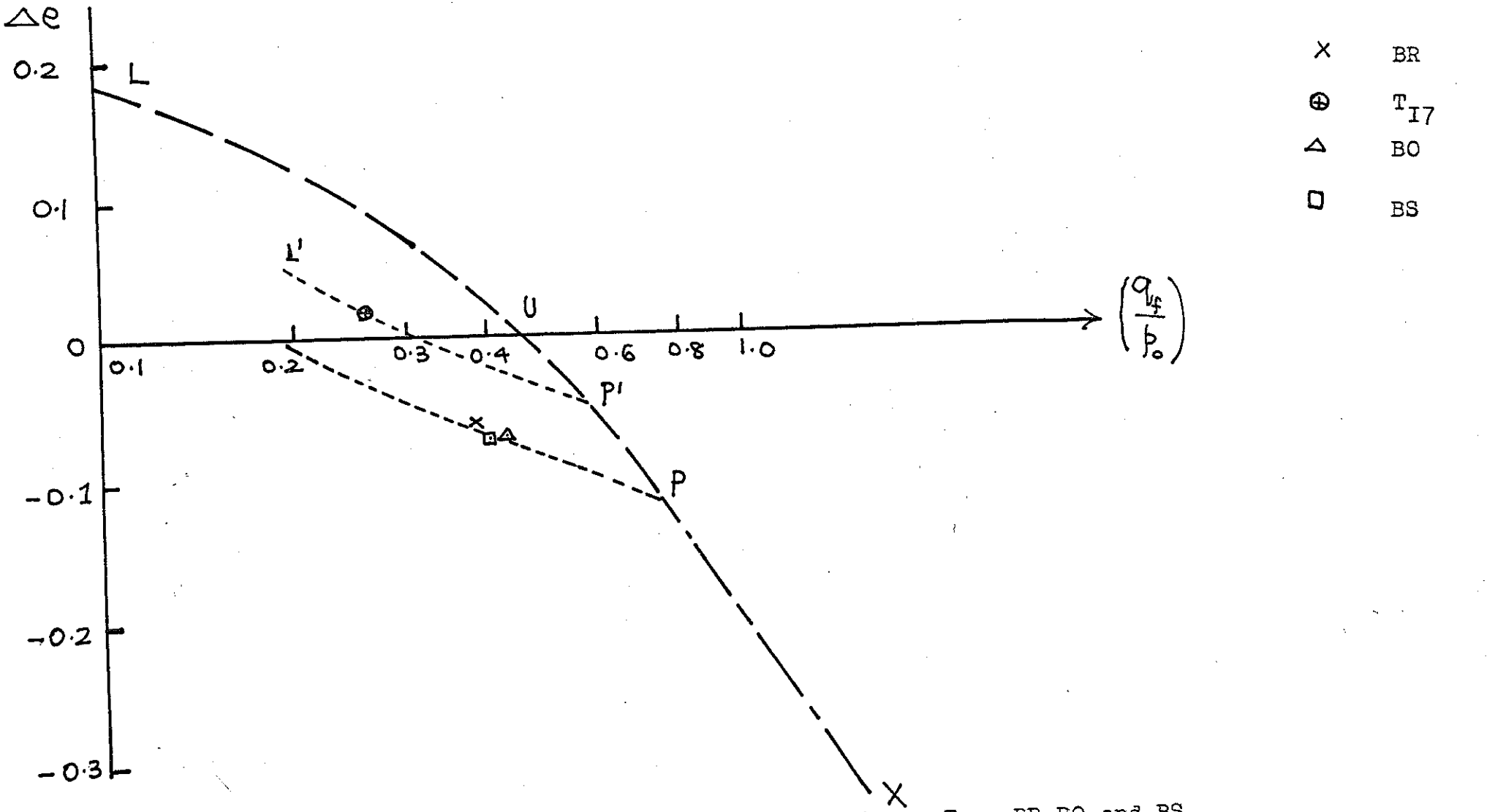

Fig. 5.3I. The (Δe, q_f/p_o) characteristics of specimens T_{I7}, BR, BO and BS.

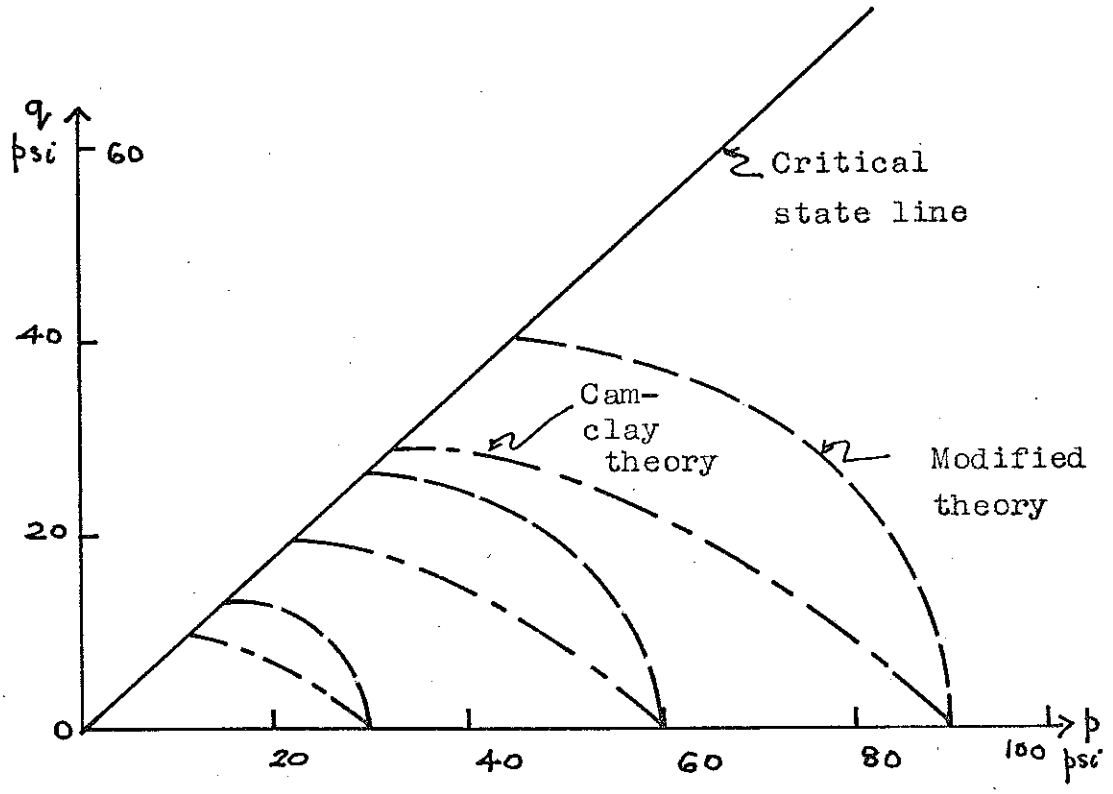

Fig. 6.1 The yield loci predicted by the Cam-clay theory and the Modified theory.

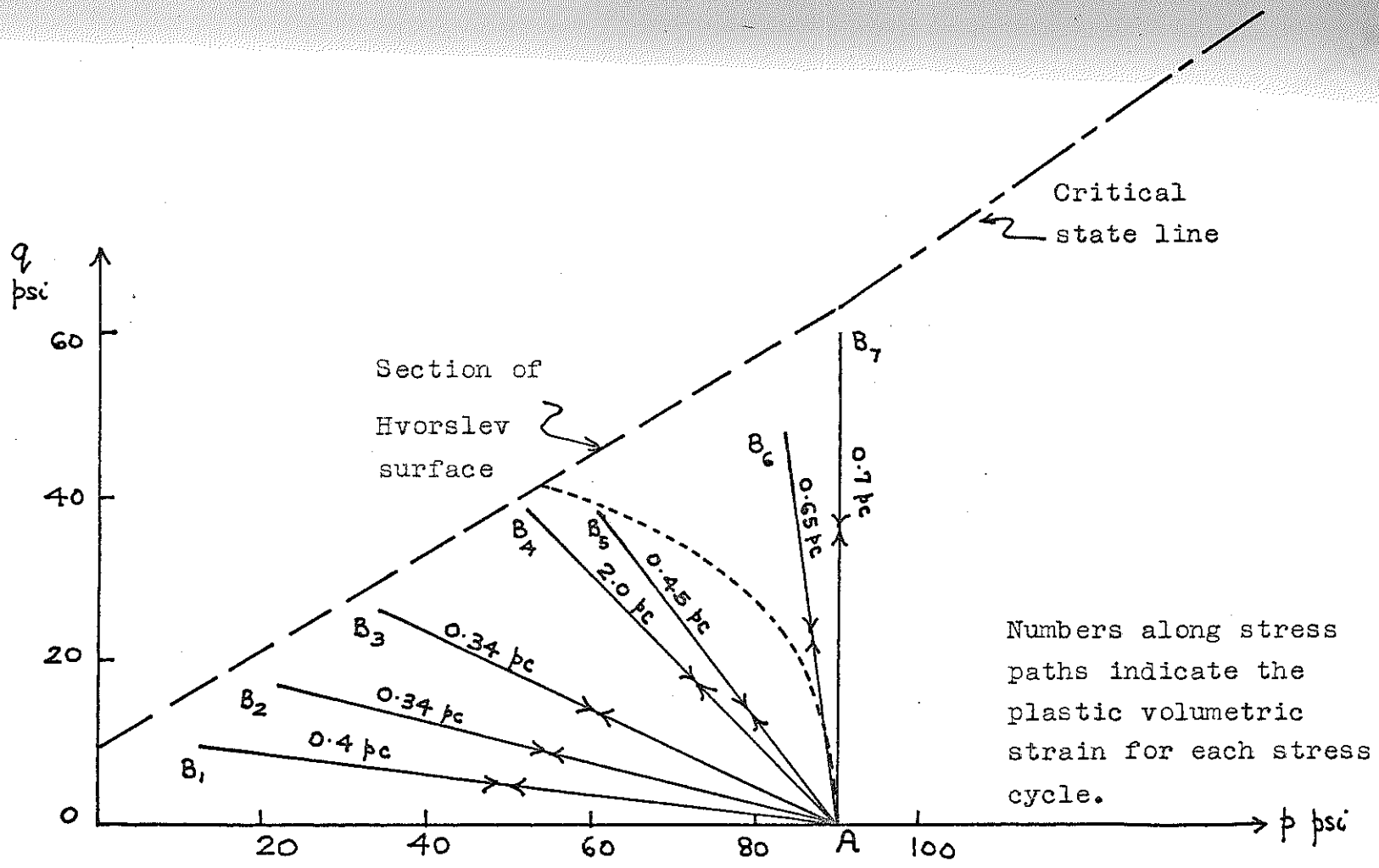

Fig. 6.2(a). The plastic volumetric strains experienced by specimen CD during stress cycles $AB_1A, AB_2A, \ldots$ and AB_7A

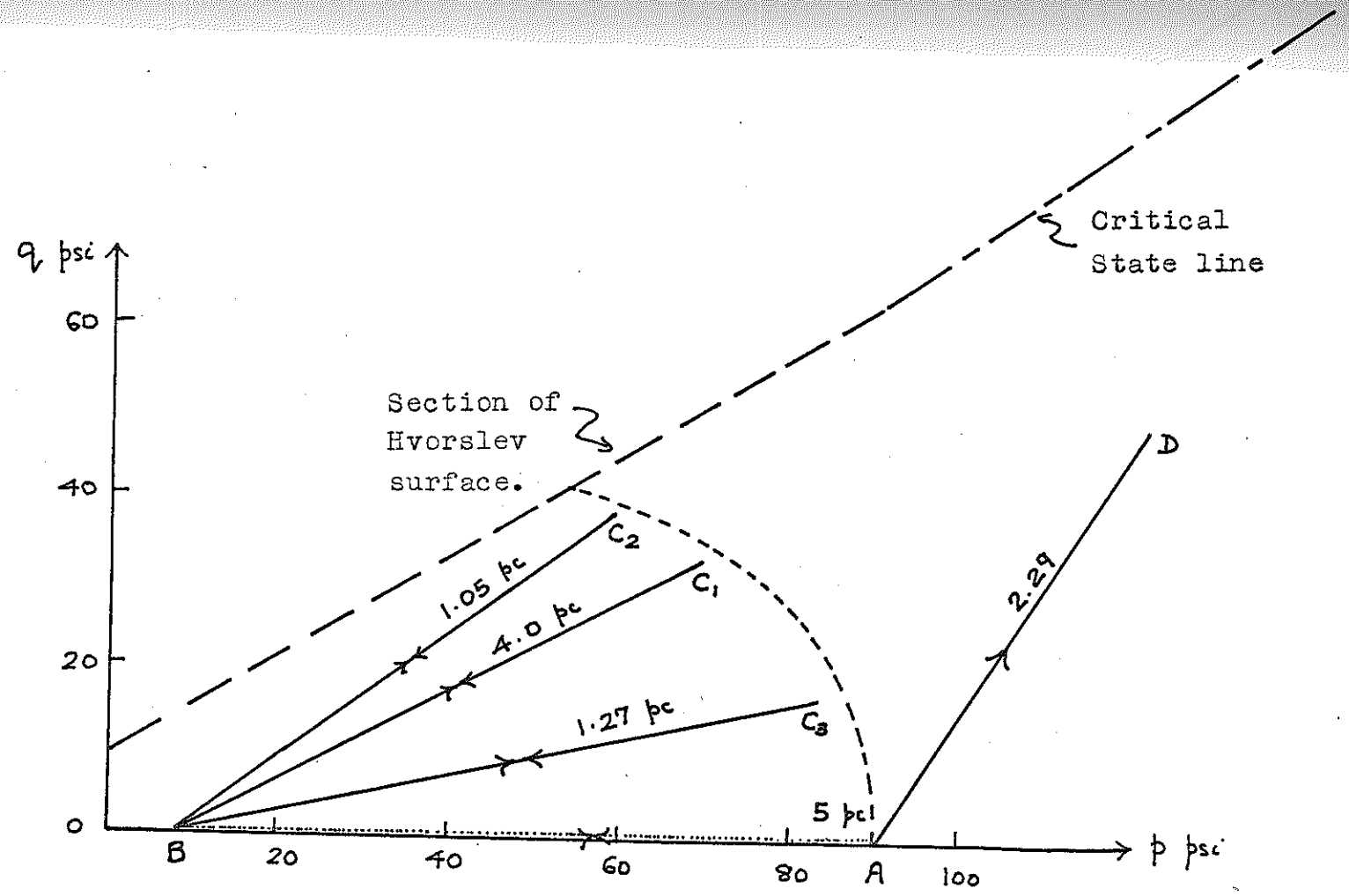

Fig. 6.2 (b) The plastic volumetric strain experienced by the heavily overconsolidated specimen T_{I9} during stress cycles BC_1B, BC_2B and BC_3B.

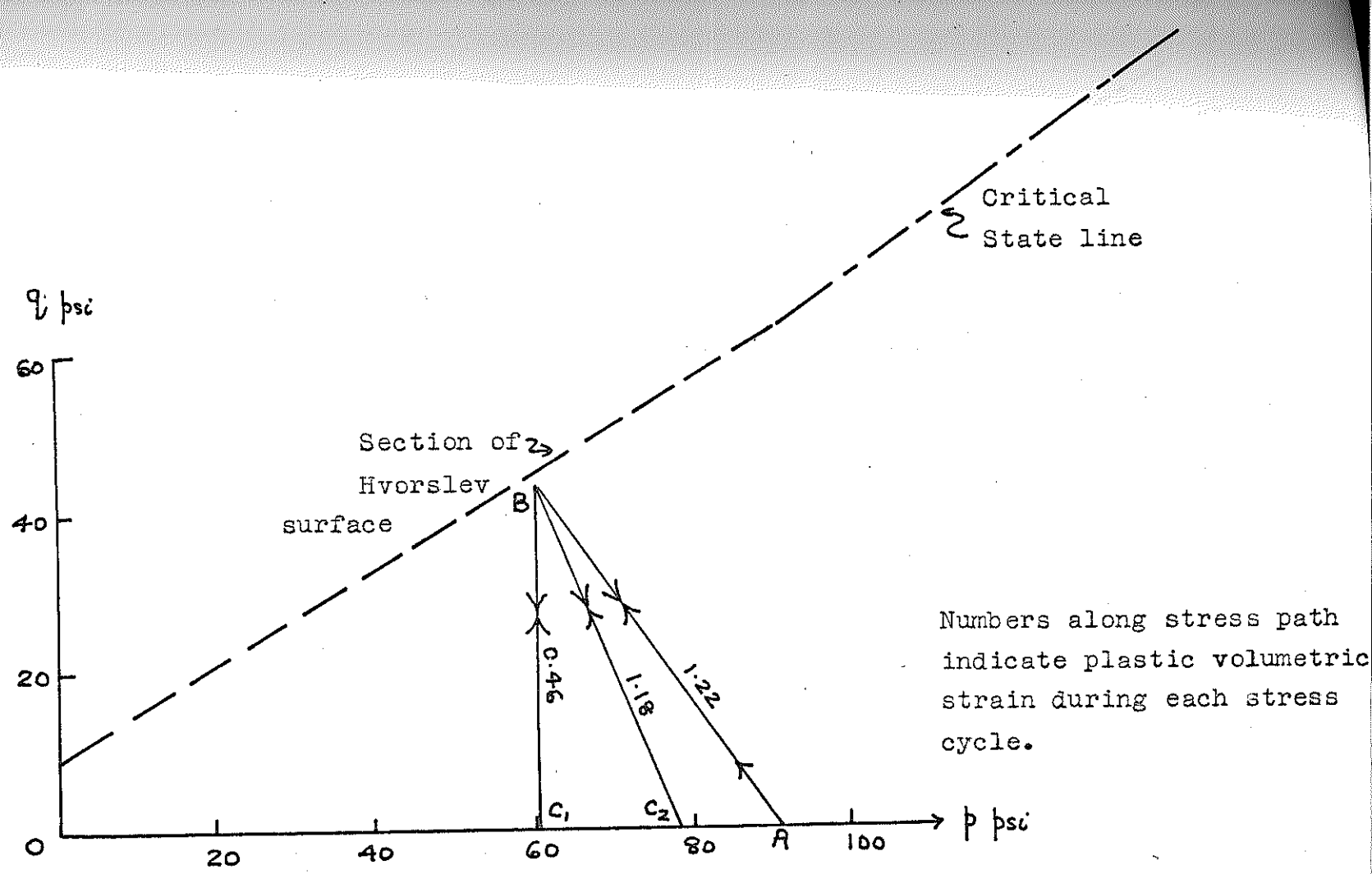

Fig. 6.2(c). The plastic volumetric strain experienced by specimen CR during stress cycles BC_1B, BC_2B and BAB.